Electronic Supplementary Material (ESI) for Metallomics.

Supporting Information-I

Cytoprotective effects of imidazole-based [S1] and [S2]-donor ligands against mercury toxicity: a bioinorganic approach

Ramesh Karri, Ashish Chalana, Ranajit Das, Rakesh Kumar Rai, Gouriprasanna Roy*

Department of Chemistry, School of Natural Sciences, Shiv Nadar University, NH91, Dadri, Gautam Buddha Nagar, UP 201314, India

Contents:

1. Synthetic Procedures:

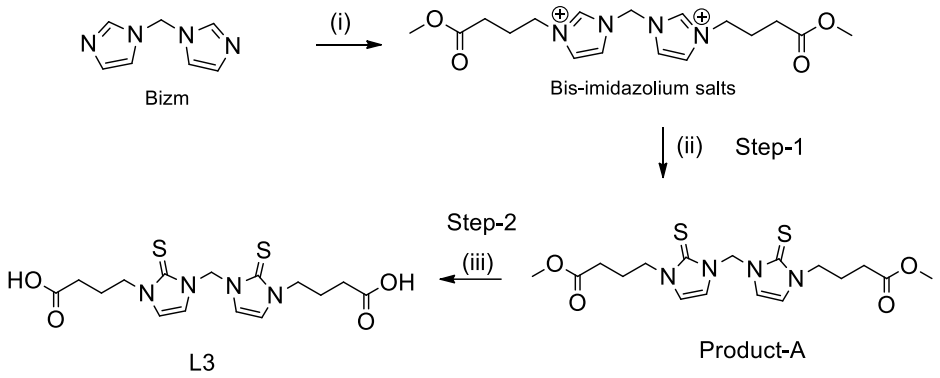

Scheme 1.Synthetic route for L3. Reagents and conditions: (i) 4-bromobutyrate, 12 h, rt (ii) K_2CO_3, dry methanol, S powder, reflux 24 h (iii) 6 N aq. NaOH, acidify with Citric acid.

Synthesis of L3 [4,4'-(3,3'-methylenebis(2-thioxo-2,3-dihydro-1H-imidazole-3,1-diyl))dibutanoic acid] :

Step 1: A 250ml two-neck round bottom flask was charged with solution of N, N-diimadazolylmethane (2g, 13.5 mmol) in acetonitrile (150 mL) and fitted with reflux condenser and septum. Ethyl-4-bromobutyrate (4.63 ml, 32.4 mmol) was slowly added and reaction mixture was heated to 96 °C for 48 h. Solvent was removed and crude was washed with ethylacetate to produce white semisolid diimadazolinium di-cationic salt. Which was dissolved in dry methanol (50 mL) then sulfur powder (1.04 g, 32.4 mmol) and anhydrous potassium carbonate (4.47g, 32.4 mmol) was added and the reaction mixture was reflux for 24 h. The solution was then filtered in hot condition through celite. Further reaction mixture was concentrate under reduced pressure and then extracted with ethylacetate and wash with brain and sodium sulphate. Reaction mixture chromatography packed with silica ethylacetate/hexane as mobile phase (0.30%).The desired **product A (L3-Ester)** was obtained as a white solid Yield: 3.83 g (69%).^{1}H NMR (400 MHz, $CDCl_3$) δ = 2.15 – 2.01 (m, 4H), 2.36 (t, *J* = 7.1 Hz, 4H), 3.66 (s, 6H), 4.06 (t, *J* = 7.2 Hz, 4H), 6.31 (s, 2H), 6.64 (d, *J* = 2.0 Hz, 2H), 7.61 (d, *J* = 2.0 Hz, 2H). ^{13C} NMR (101 MHz, CDCl3) δ = 24.2, 30.9, 47.2, 52.0, 58.1, 117.1,119.1, 163.8, 173.2. HR-ESIMS (m/z): calcd for $[M+H]^+$ $C_{17}H_{24}N_4O_4S_2$: 413.1312, observed value: 413.1310.

Step 2: Product A (1.5 g, 3.63 mmol) was dissolved in methanol (50 mL) and 6 N aq. NaOH (0.6 mL, 3.63 mmol) was added. The mixture was stirred at room temperature for about 6 h. The solvent was removed by reducing pressure to obtain salt. Which was dissolved in 5 mL of water and acidify with citric acid saturated solution at 0 °C to obtain white solid was filtered and dry under high vacuum. The desired product **L3** was obtained as a white solid. Yield: 1.18 g (85%).^{1}H NMR (DMSO-d_6) δ = 1.85 – 1.92 (m, 4H), 2.21 (t, *J* = 7.1 Hz, 4H), 3.96 (t, *J* = 7.2 Hz, 4H), 6.15 (s, 2H), 7.14 (d, *J* = 2.0 Hz, 2H), 7.40 (d, *J* = 2.0 Hz, 2H), 11.82 (s, 2H), ^{13}C NMR (DMSO-d_6) δ = 23.9, 30.7, 46.4, 55.9, 118.0,118.0, 162.5, 173.8. HR-ESIMS (m/z): calcd for $[M+H]^+$ $C_{15}H_{20}N_4O_4S_2$: 385.0999, observed value: 385.1004.

2. NMR Titrations:

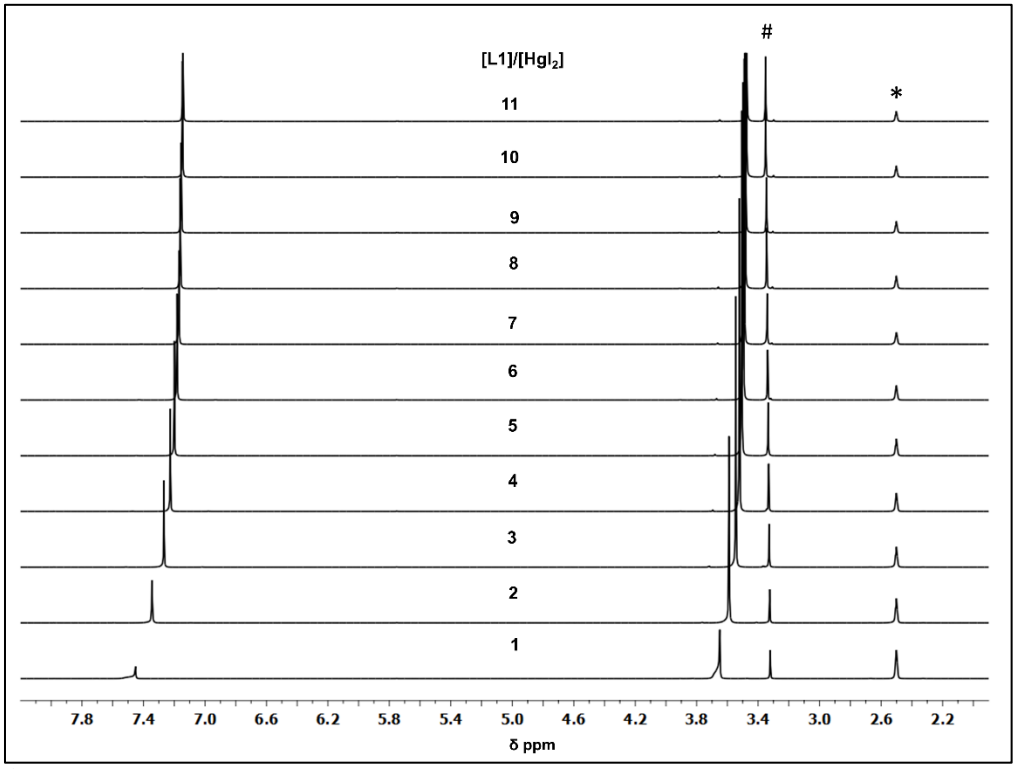

Figure S1. ^{1}H NMR titration spectra of HgI_2 (0.05 mM) with L1 from 1 to 11 equivalents in DMSO - d_6 at 21 °C (*, DMSO- d_6; #, H_2O in DMSO- d_6).

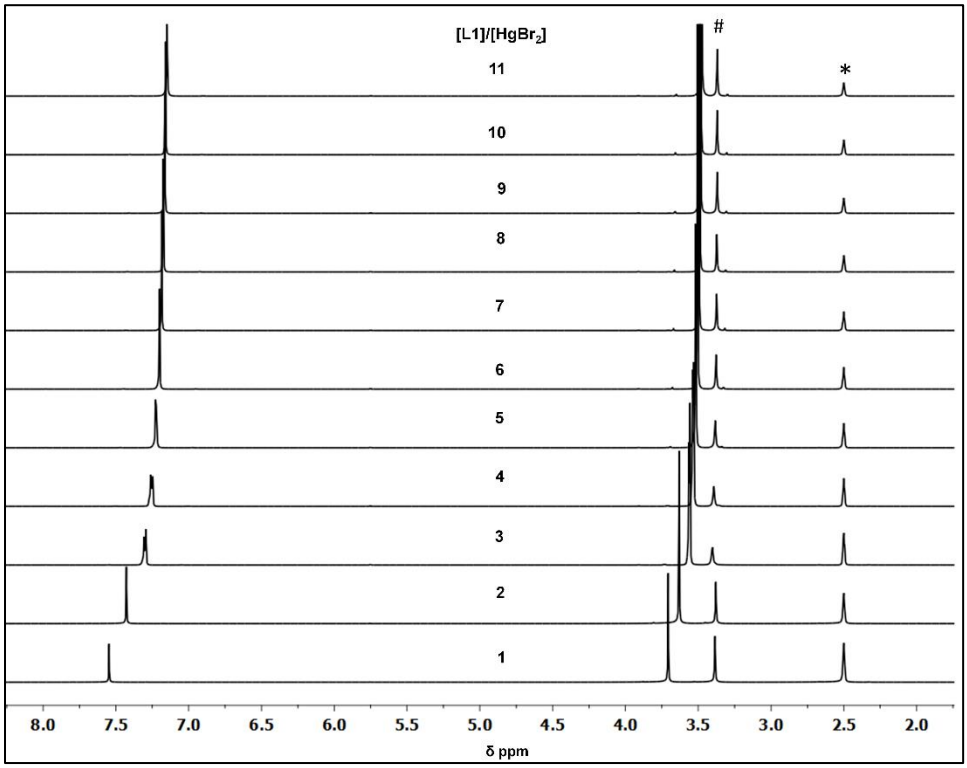

Figure S2. ^{1}H NMR titration spectra of $HgBr_2$ (0.05 mM) with L1 from 1 to 11 equivalents in DMSO - d_6 at 21 °C (*, DMSO- d_6; #, H_2O in DMSO- d_6).

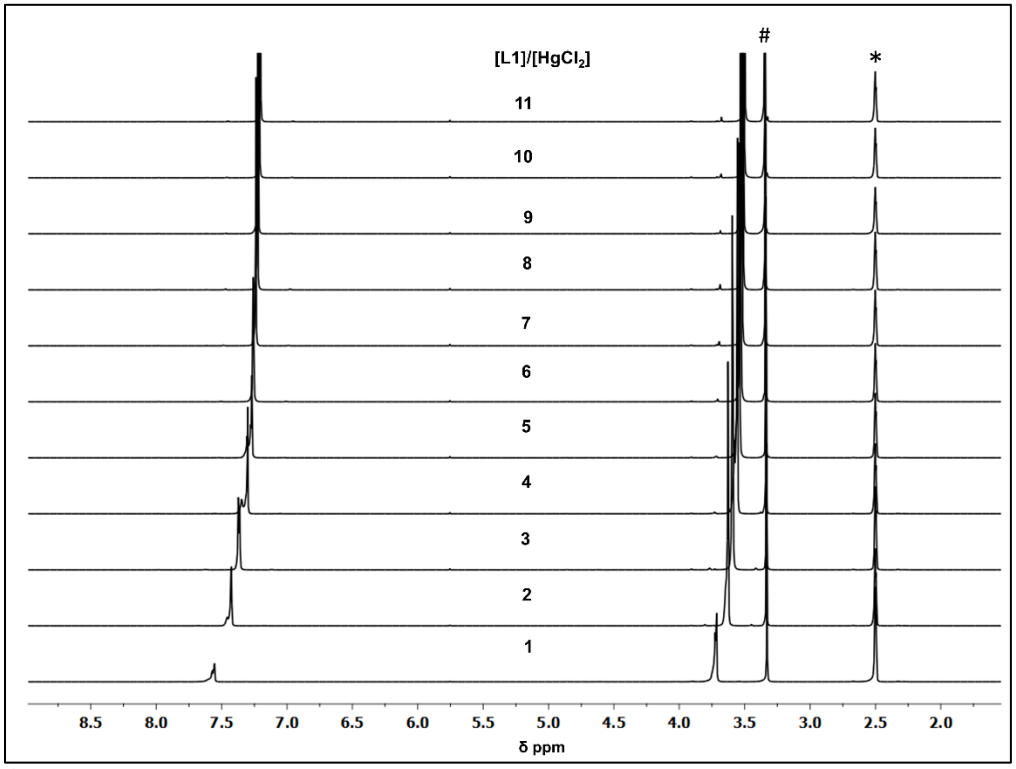

Figure S3. ^{1}H NMR titration spectra of HgI_2 (0.05 mM) with L1 from 1 to 11 equivalents in DMSO - d_6 at 21 °C (*, DMSO- d_6; #, H_2O in DMSO- d_6).

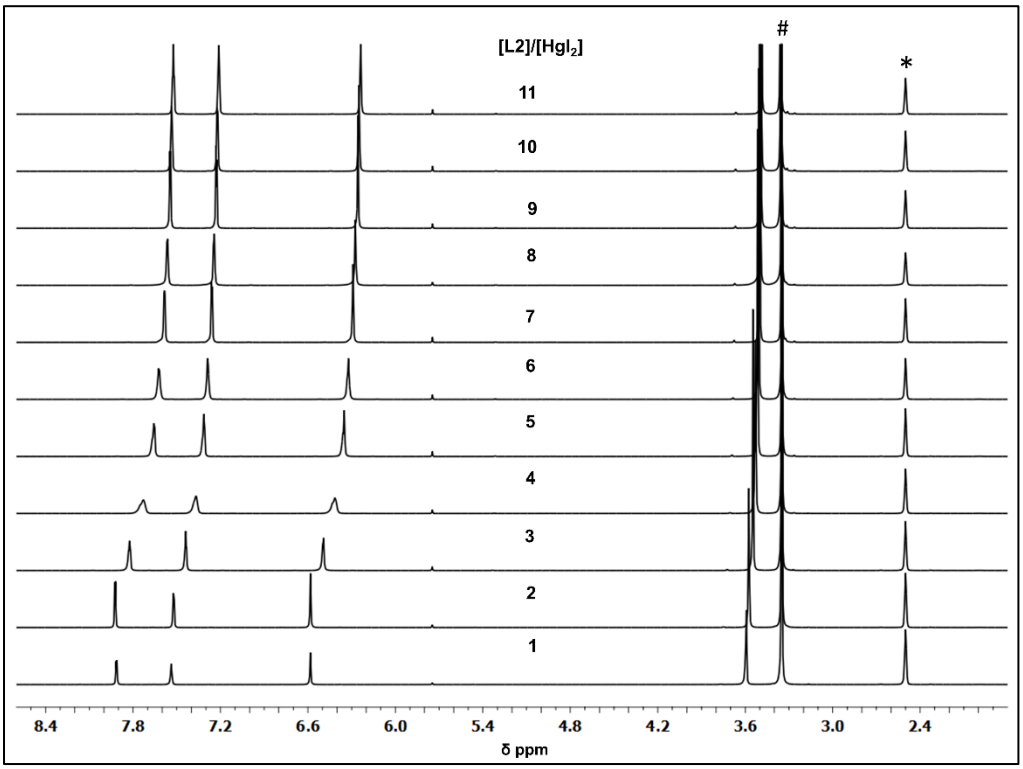

Figure S4. ^{1}H NMR titration spectra of HgI_2 (0.05 mM) with L2 from 1 to 11 equivalents in DMSO - d_6 at 21 °C (*, DMSO- d_6; #, H_2O in DMSO- d_6).

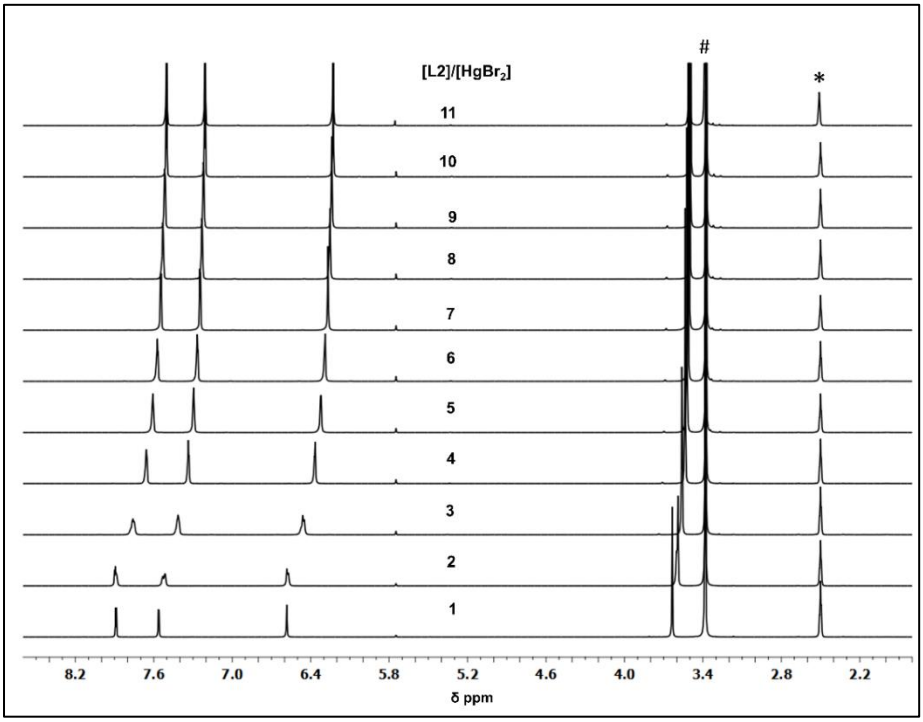

Figure S5. ^{1}H NMR titration spectra of $HgBr_2$ (0.05 mM) with L2 from 1 to 11 equivalents in DMSO - d_6 at 21 °C (*, DMSO- d_6; #, H_2O in DMSO- d_6).

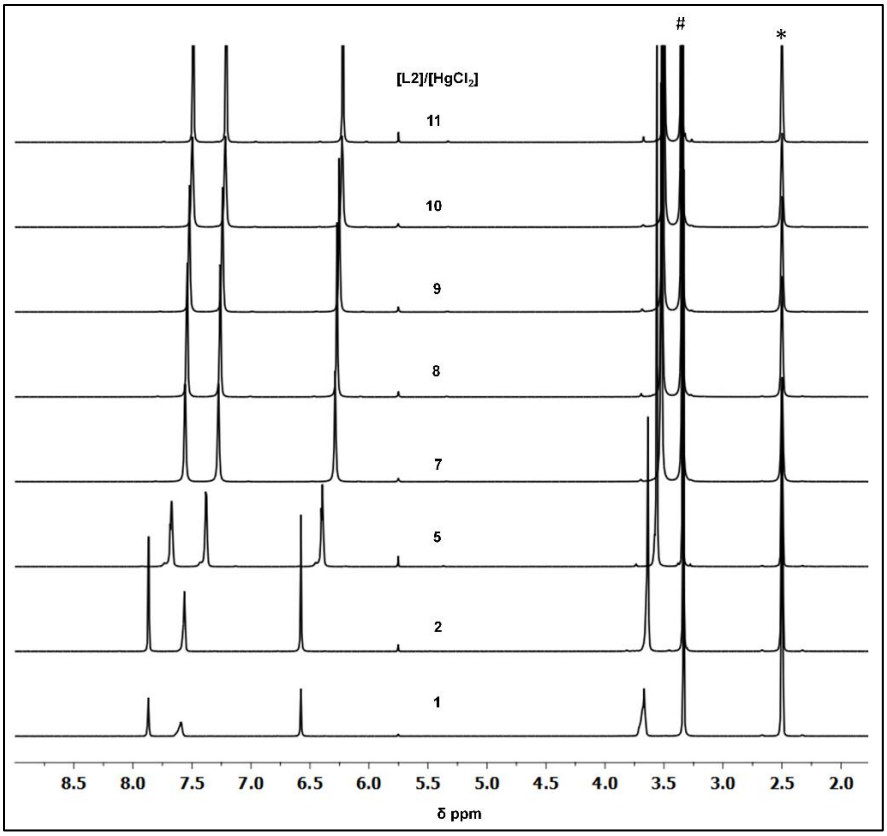

Figure S6. ^{1}H NMR titration spectra of $HgCl_2$ (0.05 mM) with L2 from 1 to 11 equivalents in DMSO - d_6 at 21 °C (*, DMSO- d_6; #, H_2O in DMSO- d_6).

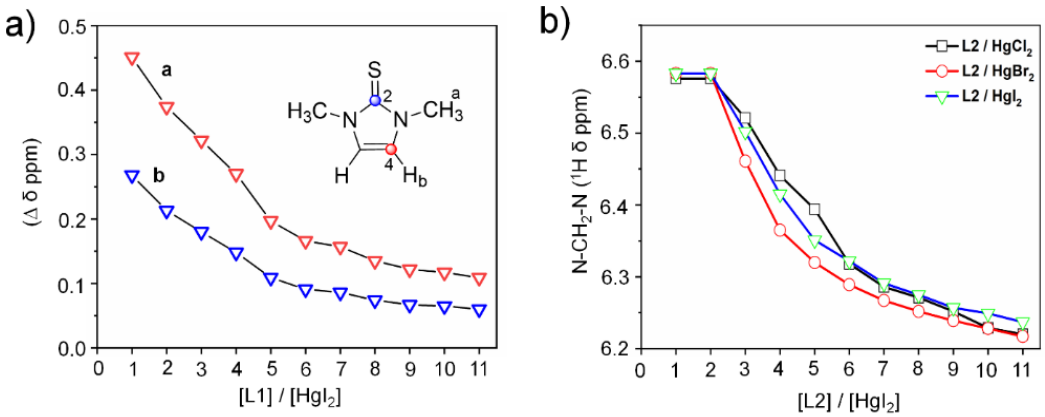

Figure S7. (a) ^{1}H NMR chemical shift of H_a (–NCH_3) & H_b (olefinic) of L1 in presence of HgI_2 (b) Change in ^{1}H NMR chemical shift of N-CH_2-N of L2 (0 to 11 equiv.) with HgX_2 (X =Cl, Br, I).

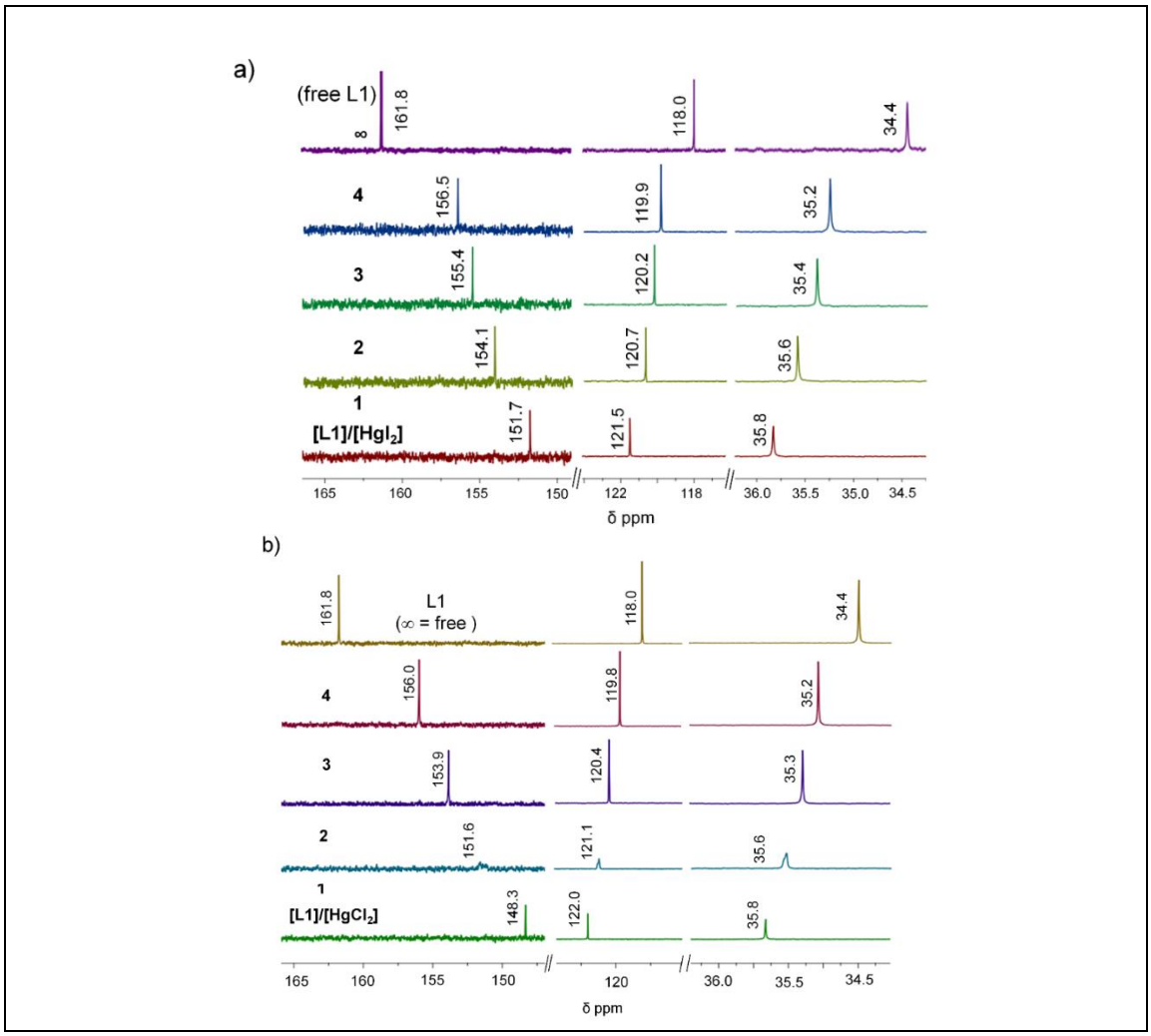

Figure S8. ^{13}C NMR chemical shift variations of L1 (1 to 4 equiv.) in the presence of (a) HgI_2 (1 equiv.) (b) $HgCl_2$ (1 equiv.) in DMSO - d_6 at 21 °C.

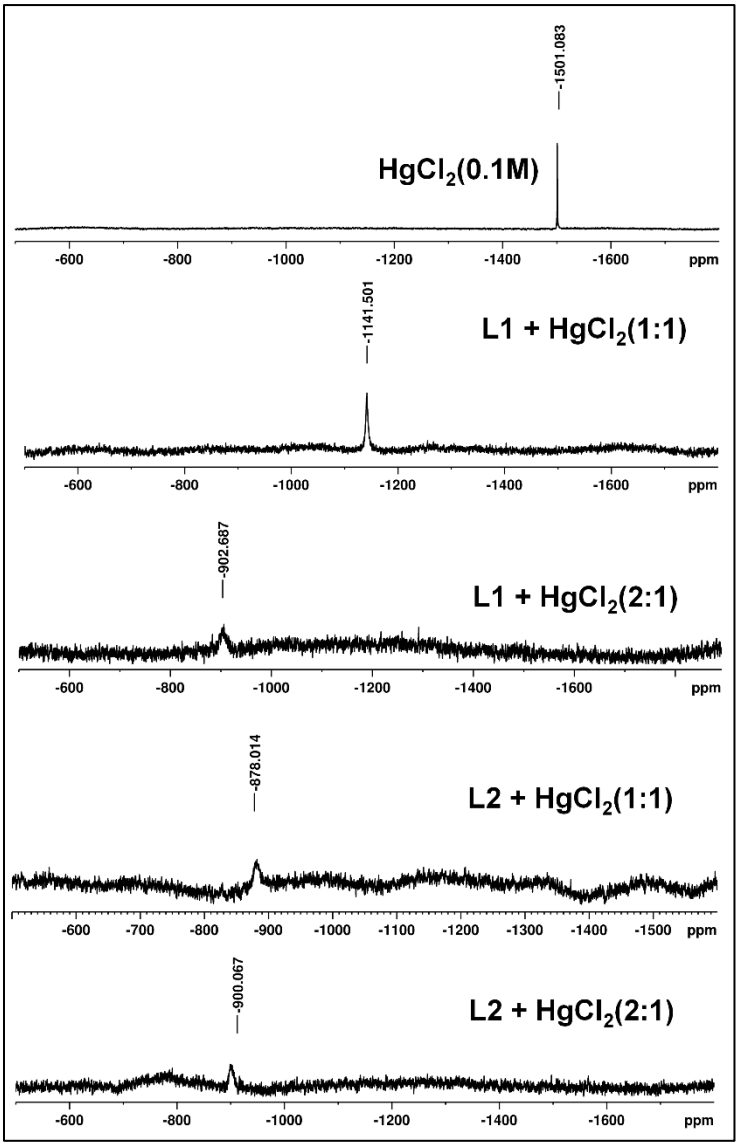

Figure S9. ^{199}Hg NMR stack spectra of $HgCl_2$ (0.1M) and, $HgCl_2$ with L1 and L2 ligand in the ratio of (1:1) & (1:2) in DMSO-d_6 at 21 °C.

3. Computational details: Geometry optimizations and frequency calculations were carried out using m062x level of theory as implemented in the Gaussians 09 package.[1] The 6-31G(d) basis set was used for all atoms (except Hg and I) whereas Stuttgart-Dresden basis set (SDD) was used for Hg and I atom with respective relativistic effective core potential.

Table S1. The C–S and C–N bond lengths of L2, k^1-$(L2)_2Hg_2Cl_4$ and k^2-$L2HgCl_2$

Compds	C-S bond length (Å)	C-N bond length (Å)
L2	1.6797	1.3564,1.3678
k^1-$(L2)_2Hg_2Cl_4$	1.7193	1.3466,1.3555
k^2-$L2HgCl_2$	1.7005	1.3511,1.3664

Table S2. Optimized geometries structures and co-ordinates.

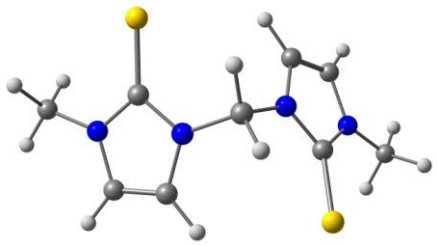

L2

16	2.539139000	1.780398000	-0.540089000
6	2.163924000	0.183611000	-0.178127000
6	1.121076000	-1.821300000	-0.049292000
1	0.325623000	-2.526629000	-0.220439000
6	2.261791000	-1.904499000	0.660025000
1	2.681079000	-2.721613000	1.219345000
6	4.157955000	-0.313373000	1.186643000
1	4.885873000	-0.063048000	0.415455000
1	4.509762000	-1.158100000	1.774622000
1	4.018353000	0.558380000	1.824943000
6	-0.000020000	0.000200000	-1.374794000
1	0.416321000	0.797564000	-1.987569000
7	1.070788000	-0.538210000	-0.571662000
7	2.895613000	-0.675140000	0.574992000
16	-2.538570000	-1.780538000	-0.539841000
6	-2.163892000	-0.183565000	-0.178145000
6	-1.121533000	1.821612000	-0.049457000
1	-0.326258000	2.527124000	-0.220659000
6	-2.262277000	1.904582000	0.659843000
1	-2.681764000	2.721633000	1.219106000
6	-4.157973000	0.312975000	1.186714000
1	-4.885850000	0.062337000	0.415589000
1	-4.510002000	1.157674000	1.774600000
1	-4.018089000	-0.558656000	1.825119000
1	-0.416333000	-0.797170000	-1.987576000
7	-1.070935000	0.538492000	-0.571729000
7	-2.895770000	0.675042000	0.574952000

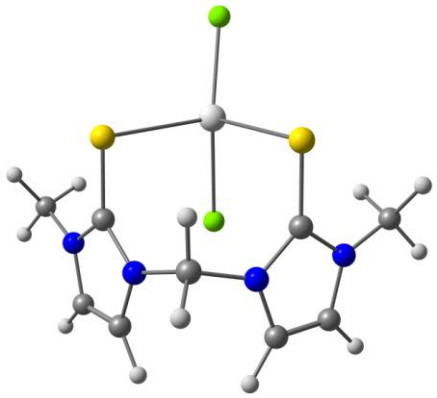

k^2-L2HgCl$_2$

80	-1.423726000	0.000005000	-0.151667000
16	-0.274555000	-1.938727000	1.523008000
7	1.472162000	-2.877825000	-0.341266000
7	2.281575000	-1.201759000	0.763272000
6	1.174383000	-1.992051000	0.634550000
6	0.508120000	-3.819874000	-0.886855000
1	1.039408000	-4.515424000	-1.536700000
1	-0.244554000	-3.270622000	-1.459592000
1	0.023616000	-4.355188000	-0.070201000
6	3.251406000	-1.605899000	-0.140344000
1	4.219540000	-1.137119000	-0.198527000
6	2.739866000	-2.646170000	-0.832015000
1	3.161833000	-3.245162000	-1.622759000
16	-0.274539000	1.938730000	1.523006000
7	1.472187000	2.877816000	-0.341265000
7	2.281586000	1.201743000	0.763272000
6	1.174400000	1.992043000	0.634549000
6	0.508154000	3.819873000	-0.886855000
1	1.039448000	4.515418000	-1.536700000
1	-0.244525000	3.270627000	-1.459592000
1	0.023655000	4.355192000	-0.070201000
6	3.251420000	1.605875000	-0.140343000
1	4.219551000	1.137088000	-0.198524000
6	2.739890000	2.646149000	-0.832015000
1	3.161862000	3.245138000	-1.622758000
17	-3.826885000	0.000014000	-0.058342000
17	0.454333000	-0.000004000	-1.816022000
6	2.358973000	-0.000009000	1.573515000
1	3.308499000	-0.000013000	2.114187000
1	1.516399000	-0.000005000	2.269460000

80	3.761880000	0.000848000	0.380606000
17	6.168845000	0.001115000	-0.159732000
16	2.817029000	2.248248000	1.533165000
17	2.177381000	0.000591000	-1.665945000
7	1.075386000	2.779123000	-0.539429000
7	3.094906000	3.445304000	-0.920889000
6	2.317782000	2.842296000	-0.001118000
6	-0.000546000	1.974154000	-0.000023000
1	-0.405028000	1.348644000	-0.796430000
6	2.346527000	3.744079000	-2.043875000
1	2.786971000	4.218649000	-2.905626000
6	4.535861000	3.622814000	-0.779431000
1	4.749541000	4.080138000	0.187092000
1	4.877842000	4.269814000	-1.587033000
1	5.039725000	2.652393000	-0.838845000

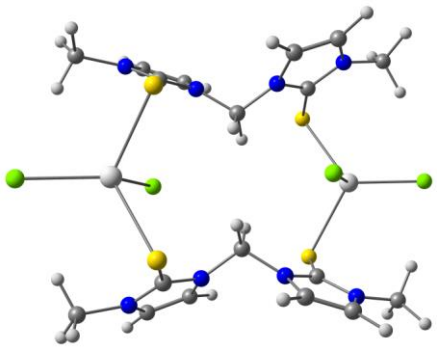

k^l-(L2)$_2$Hg$_2$Cl$_4$

6	1.082206000	3.323773000	-1.808522000
1	0.191786000	3.336425000	-2.418665000
16	-2.818011000	2.246947000	-1.533607000
7	-1.076792000	2.778919000	0.539050000
7	-3.096543000	3.444644000	0.920075000
6	-2.319155000	2.841522000	0.000598000
1	0.404173000	1.349127000	0.796641000
6	-2.348381000	3.743951000	2.043064000
1	-2.789052000	4.218686000	2.904608000
6	-4.537515000	3.621829000	0.778360000
1	-4.751148000	4.078754000	-0.188363000
1	-4.879718000	4.269078000	1.585670000
1	-5.041218000	2.651346000	0.838074000
6	-1.083914000	3.323938000	1.807983000
1	-0.193566000	3.337034000	2.418221000
80	-3.762135000	-0.000737000	-0.380835000
17	-6.169154000	-0.001128000	0.159258000
17	-2.177826000	-0.000259000	1.665865000
16	-2.817067000	-2.248065000	-1.533435000
7	-1.075609000	-2.779294000	0.539193000
7	-3.095195000	-3.445349000	0.920492000
6	-2.317976000	-2.842318000	0.000819000
6	0.000365000	-1.974307000	-0.000090000
1	0.404802000	-1.348849000	0.796380000
6	-2.346883000	-3.744329000	2.043470000
1	-2.787402000	-4.218961000	2.905148000
6	-4.536162000	-3.622691000	0.778964000
1	-4.749856000	-4.079844000	-0.187636000
1	-4.878236000	-4.269780000	1.586457000
1	-5.039923000	-2.652224000	0.838508000
6	-1.082525000	-3.324067000	1.808231000
1	-0.192137000	-3.336833000	2.418419000
16	2.817775000	-2.246787000	1.533496000
7	1.076652000	-2.779023000	-0.539148000
7	3.096496000	-3.444442000	-0.920180000
6	2.319004000	-2.841502000	-0.000677000
1	-0.404311000	-1.349223000	-0.796732000
6	2.348365000	-3.743913000	-2.043146000
1	2.789107000	-4.218568000	-2.904697000
6	4.537512000	-3.621283000	-0.778505000
1	4.751275000	-4.078212000	0.188187000
1	4.879862000	-4.268395000	-1.585863000
1	5.040962000	-2.650664000	-0.838166000
6	1.083844000	-3.324051000	-1.808075000
1	0.193505000	-3.337235000	-2.418328000

4. UV-vis spectroscopic analysis:

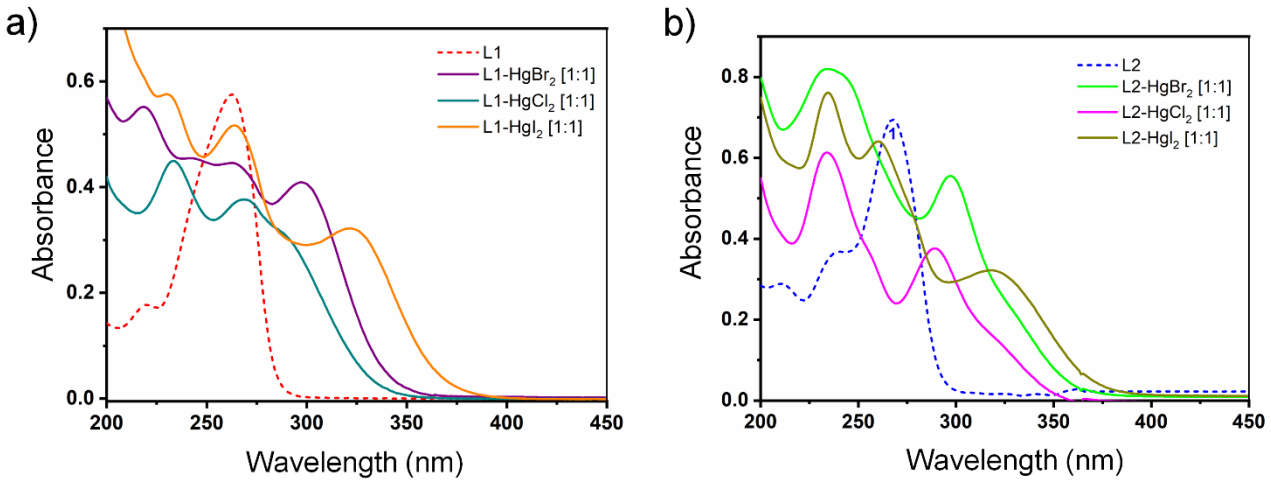

Figure S10. UV-vis spectra of 5 x 10^{-5} M solutions of (a) L1 with HgX_2, (b) L2 with HgX_2 in acetonitrile (where X = Cl, Br, I).

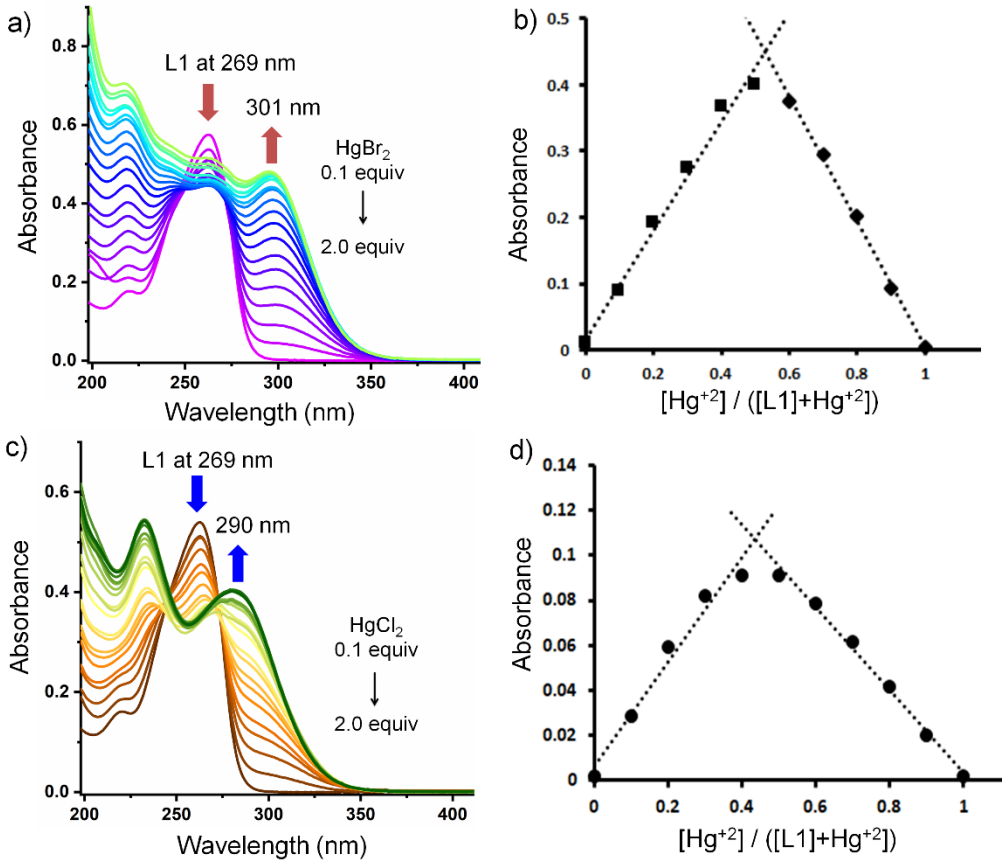

Figure S11. (a) & (c) UV-vis titration profile of L1 (5 x 10^{-5} M) with 0.1 to 2 equiv. of $HgBr_2$ and $HgCl_2$, (b) & (d) Job's plot of the L1 with $HgBr_2$ and $HgCl_2$ in acetonitrile at 301nm, 290 nm respectively.

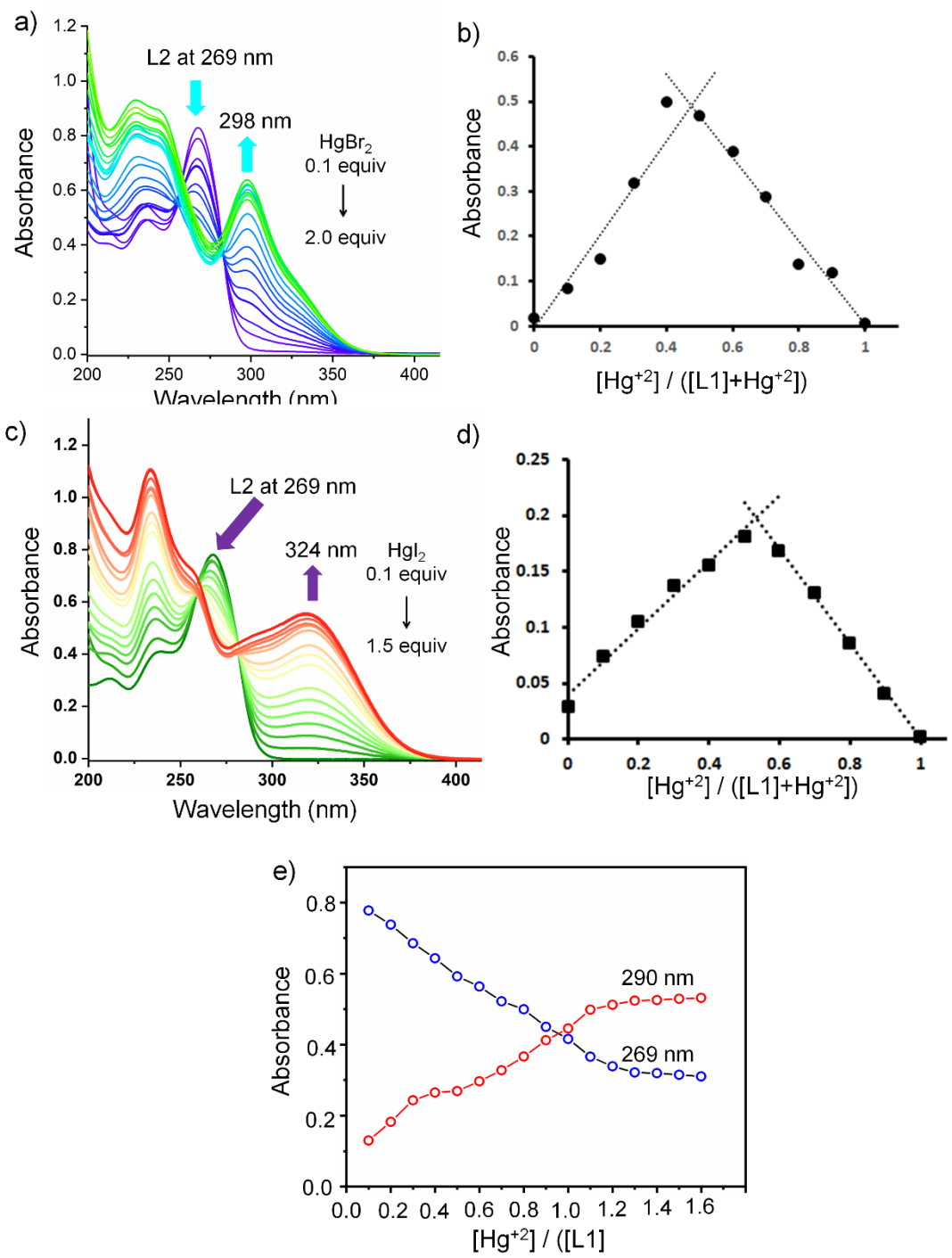

Figure S12. (a) & (c) UV-vis titration profile of L2 (5 x 10^{-5} M) with 0.1 to 2 equiv. of $HgBr_2$ and HgI_2, (b) & (d) Job's plot of the L2 with $HgBr_2$ and HgI_2 in acetonitrile at 301nm, 290 nm respectively, (e) The titration curves of the L2 with $HgCl_2$.

5. X-ray Crystallography Analysis:

Table S3. Crystallographic data for $[(L1)_2HgBr_2]$, $[(L1HgI_2)_2]$ and $[(L1)_3Hg_2I_4]$.

	$(L1)_2HgBr_2$	$(L1HgI_2)_2$	$(L1)_3Hg_2I_4$
CCDC no.	1486402	1857557	1857558
Lattice	Monoclinic	Monoclinic	Monoclinic
Formula	C10 H16 Br2 Hg N4 S2	C10 H16 Hg2 I4 N4 S2	C15 H24 Hg2 I4 N6 S3
Formula Weight	616.78	1165.17	1293.36
Space Group	*P21/n*	*C2/m*	*P21/c*
a/ A°	9.6186(7)	10.1454(3)	18.3607(7)
b/ A°	14.2021(11)	15.0815(3)	14.7466(6)
c/ A°	13.5419(11)	15.0815(3)	11.7959(4)
α/ °	90	90	90
β/ °	108.982(3)	90	107.761(1)
γ/ °	90	90	90
V/ $A^{\circ 3}$	1749.3(2)	2340.94(10)	3041.6(2)
Z	4	4	4
Temperature (K)	252 K	296 K	273 K
Radiation (λ)/A°	0.71073	0.71073	0.71073
ρ/ (g cm^{-3})	2.342	3.306	2.824
μ (Mo K_α) mm^{-1}	13.598	18.554	14.364
θ_{max}/deg	26.415	25.676	25.681
No. of data collected	3582	2219	35205
No. of data	3083	1990	5765
No. of parameters	177	103	272
R_1 [I> 2σI]	0.0262	0.0212	0.0322
wR_2 [I> 2σI]	0.0590	0.0445	0.0544
R_1 [all data]	0.0348	0.0262	0.0567
wR_2 [all data]	0.0622	0.0467	0.0657
R_{int} [all data]	0.0779	0.0320	0.0516
GOF	1.030	1.061	1.063

Table S4. Crystallographic data for L3, $(L2)_2Hg_2Cl_4$.DMSO, $(L2)_2Hg_2Br_4$, $[L2Hg_2I_4]_n$.

	L3	k^l-$(L2)_2Hg_2Cl_4$. DMSO	k^l-$(L2)_2Hg_2Br_4$	k^l-$[L2Hg_2I_4]_n$
CCDC no.	1857559	1534013	1857556	1857560
Lattice	Monoclinic	Monoclinic	Monoclinic	Monoclinic
Formula	C15 H20 N4 O4 S2	$C_{22}H_{36}Cl_4Hg_2N_8O_2S_6$	C18 H24 Br4 Hg2 N8 S4	C9 H12 Hg2 I4 N4 S2
Formula Weight	384.47	1179.93	1201.47	1149.13
Space Group	C 2/c	C 2/m	*C2/m*	C 2/c
a/ A°	7.2921(6)	17.9245(16)	17.7977(16)	38.111(3)
b/ A°	7.8235(6)	12.3888(16)	12.2950(11)	7.4534(5)
c/ A°	30.636(2)	10.6773(10)	10.8212(10)	16.3979(13)
α/ °	90	90	90	90
β/ °	93.610(3)	126.485(5)	125.868(2)	113.273(2)
γ/ °	90	90	90	90
V/ $A^{\circ 3}$	1744.3(2)	1906.3(4)	1918.9(3)	4278.9(6)
Z	4	2	2	8
Temperature (K)	298	298	298K	297 K
Radiation (λ)/A°	0.71073	0.71073	0.71073	0.71073
ρ/ (g cm^{-3})	1.464	2.056	2.079	3.568
μ (Mo K_α) mm^{-1}	0.334	8.687	12.393	20.299
θ_{max}/deg	26.372	26.362	26.367	26.022
No. of data collected	13043	36936	15576	38595
No. of data	1795	1993	1545	3245
No. of parameters	115	119	88	203
R_1 [I> 2σI]	0.0419	0.0275	0.0354	0.0383
wR_2 [I> 2σI]	0.0878	0.0722	0.0938	0.0738
R_1 [all data]	0.0563	0.0290	0.0573	0.0576
wR_2 [all data]	0.0957	0.0729	0.1099	0.0798
R_{int} [all data]	0.0375	0.0476	0.0682	0.055
GOF	1.093	1.336	0.757	1.028

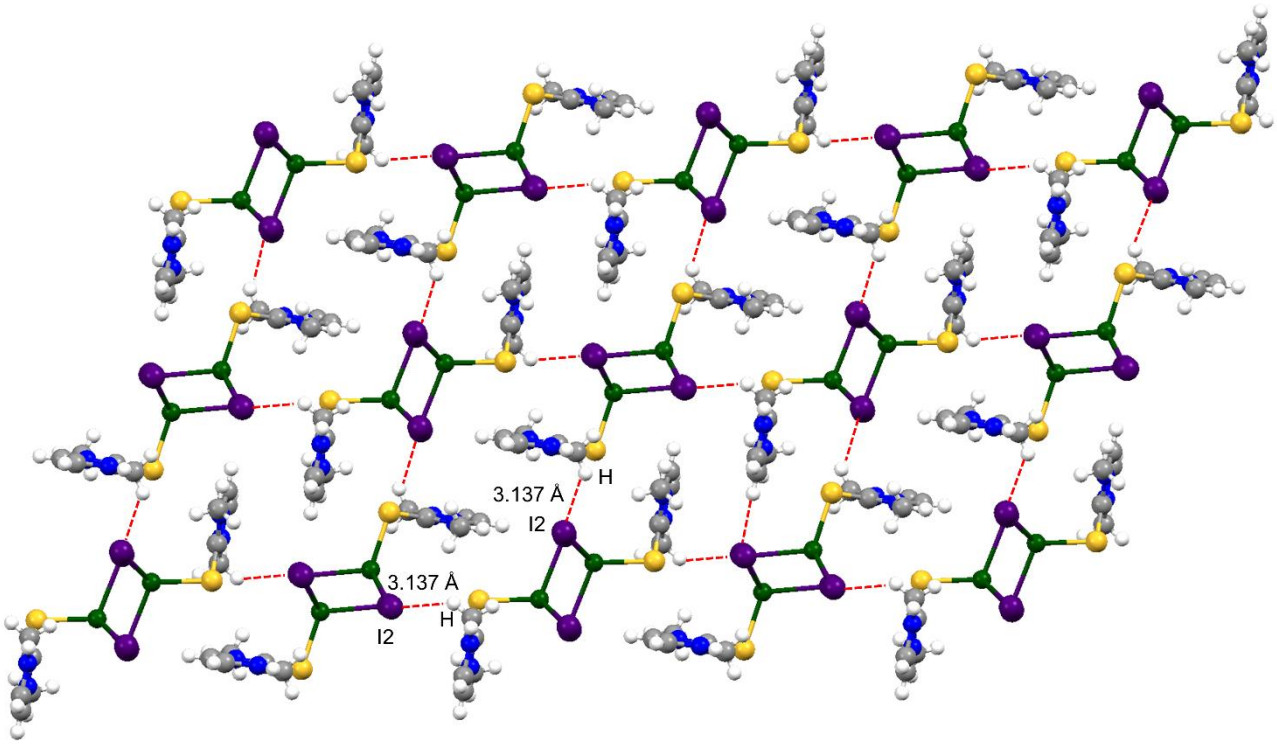

Figure S13. The crystal packing of $(L1)_2Hg_2I_4$ (drawn in Mercury 3.8 software) showing shows that intermolecular hydrogen bonding between the H atom of $–NCH_3$ hydrogen with bridged iodine atom ($d_{(H\cdots I2)}$: 3.137 Å).

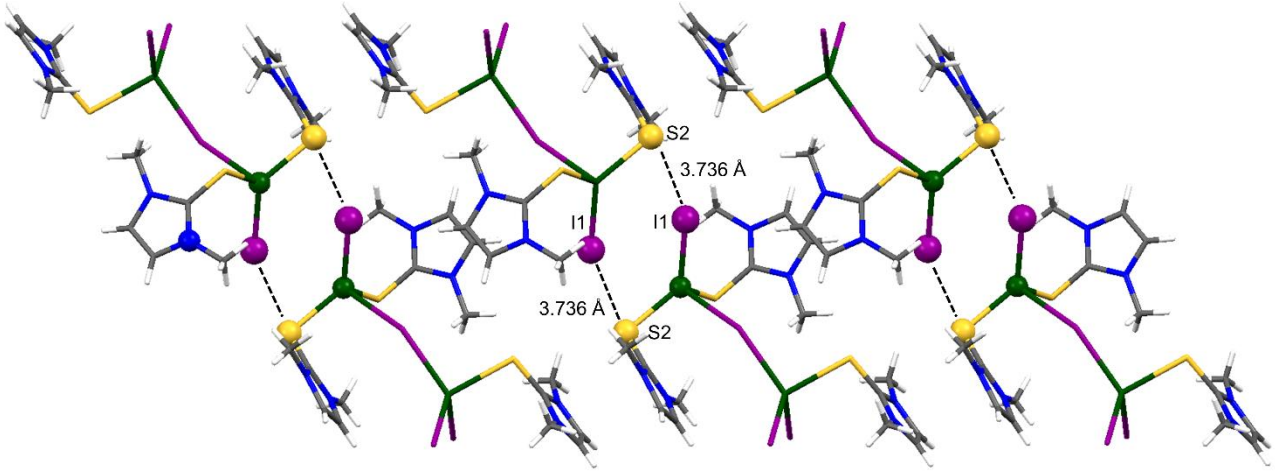

Figure S14. The crystal packing of $(L1)_3Hg_2I_4$ (drawn in Mercury 3.8 software) showing a chain like structure with intermolecular S2···I1 interactions ($d_{(H\cdots I2)}$: 3.736 Å).

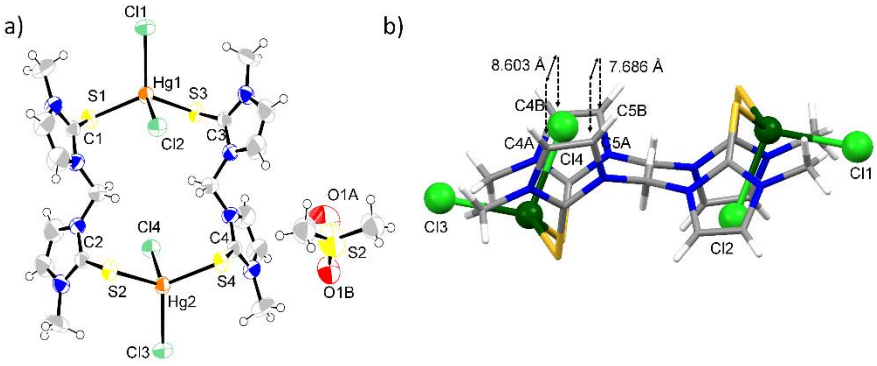

Figure S15. (a) ORTEP images of k^1-$(L2)_2Hg_2Cl_4$ with solvent molecule DMSO. (b) Molecular structure of k^1-$(L2)_2Hg_2Cl_4$ showing the orientation of Cl atoms in the molecule.

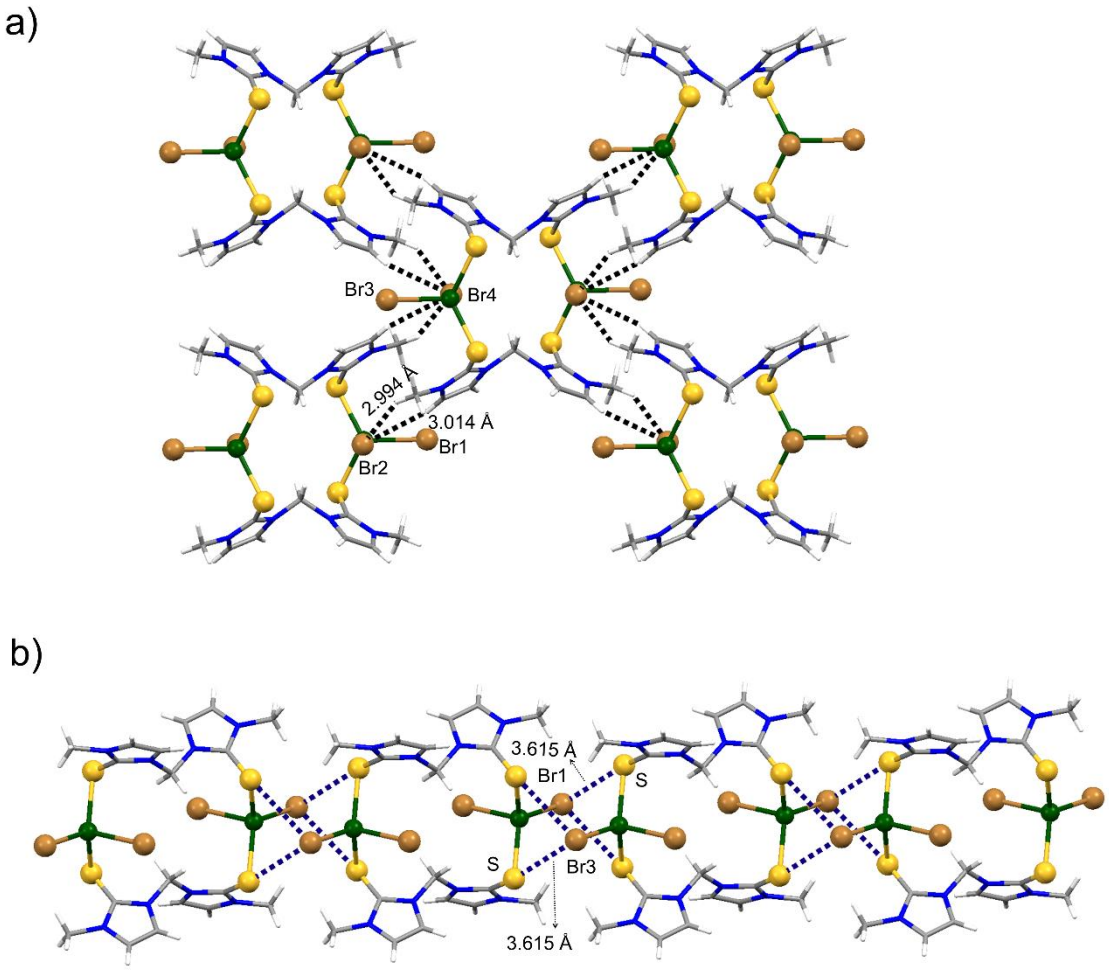

Figure S16. The crystal packing of k^1-$(L2)_2Hg_2Br_4$ metallacycle (drawn in Mercury 3.8 software) showing (a) Intermolecular hydrogen bonding interactions between two bromine atoms (Br2 & Br4) and the H atom of –NMe, and olefinic H atom [or imidazole -CH] of two different metallacycles with distance $d_{(H\text{-}Br2)} = d_{(H\text{-}Br4)} = 2.994$ Å & $d_{(H\text{-}Br2)} = d_{(H\text{-}Br4))} = 3.014$ Å. (b) The other two bromine atoms (Br1 & Br3) showing intermolecular S···Br1 interactions ($d_{(S\text{-}Br2)} = d_{(S\text{-}Br3)} = 3.615$ Å).

6. ^{1}H and ^{13}C NMR spectra

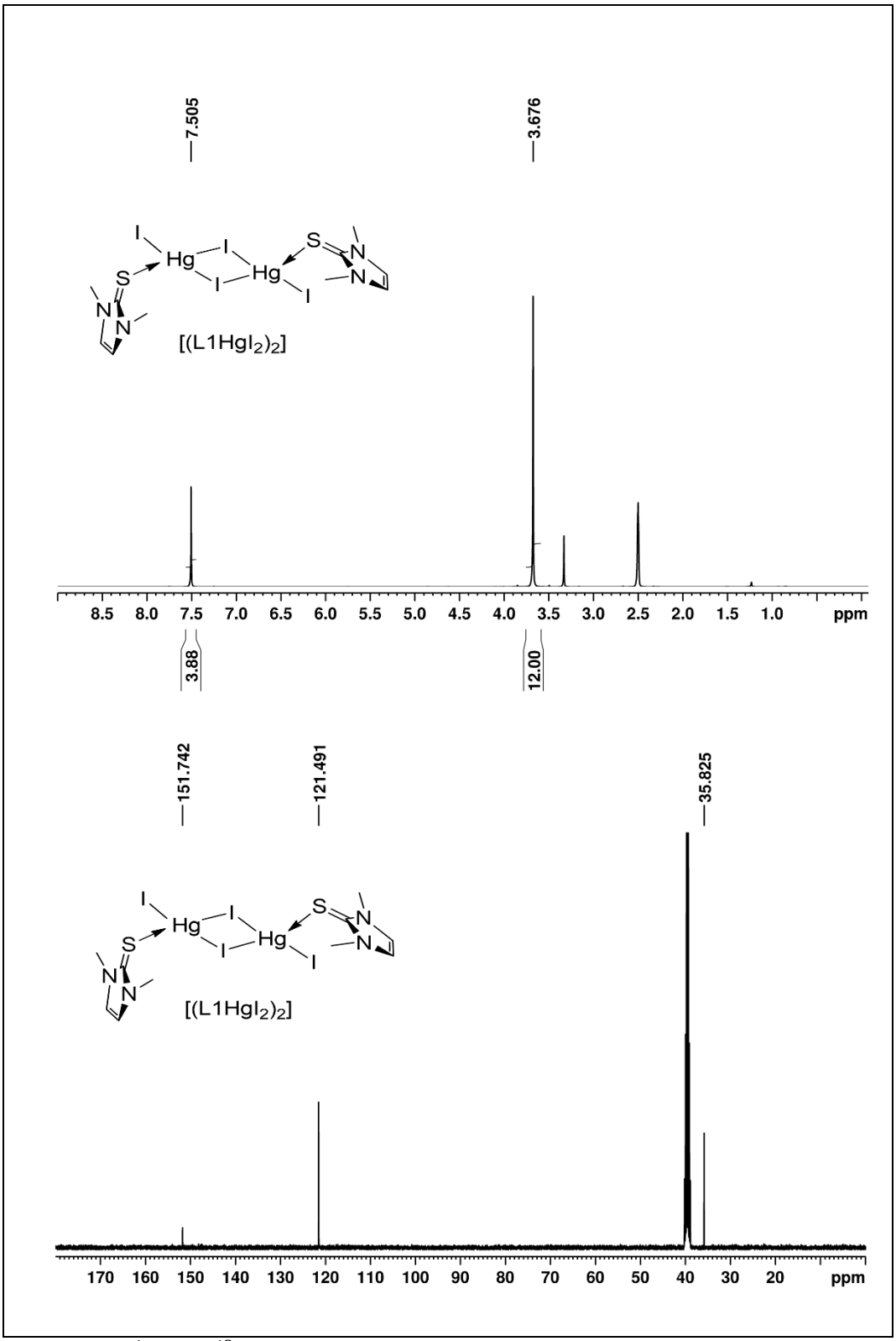

Figure S17. ^{1}H and ^{13}C NMR spectra of $(L1)_2Hg_2I_4$ in DMSO-*d*$_6$.

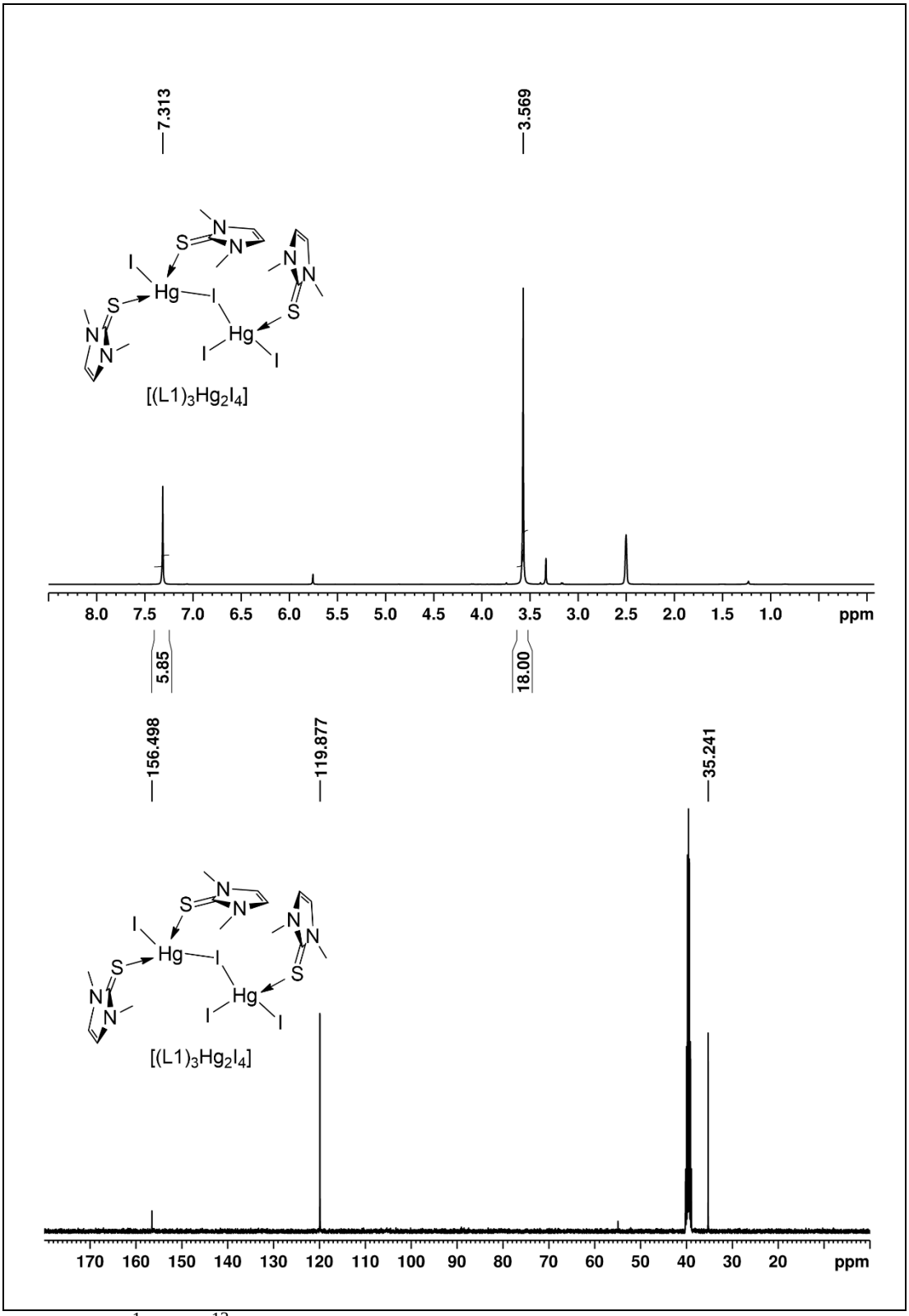

Figure S18. ^{1}H and ^{13}C NMR spectra of $(L1)_3Hg_2I_4$ in DMSO-d_6.

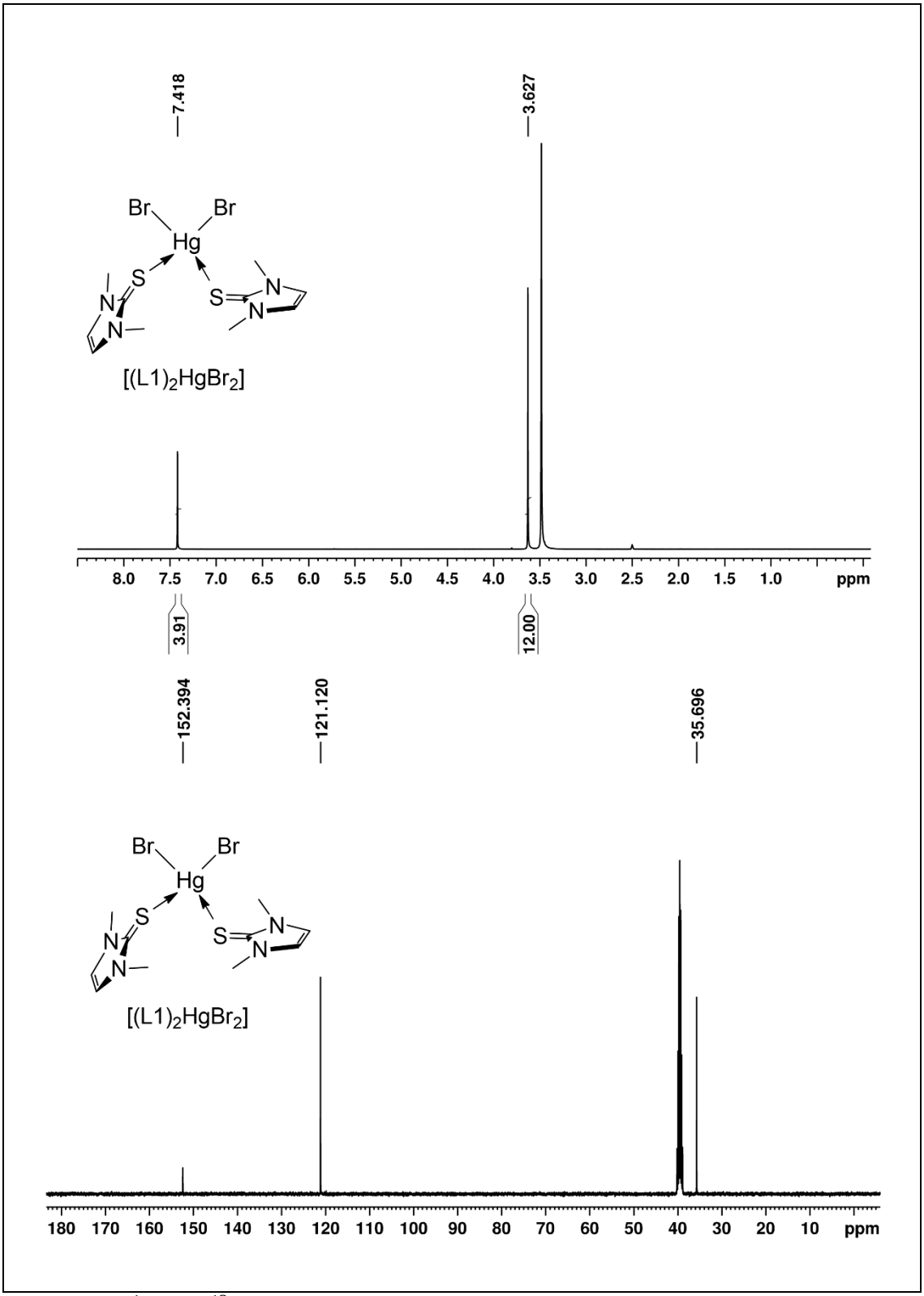

Figure S19. ^{1}H and ^{13}C NMR spectra of $(L1)_2HgBr_2$ in DMSO-d_6.

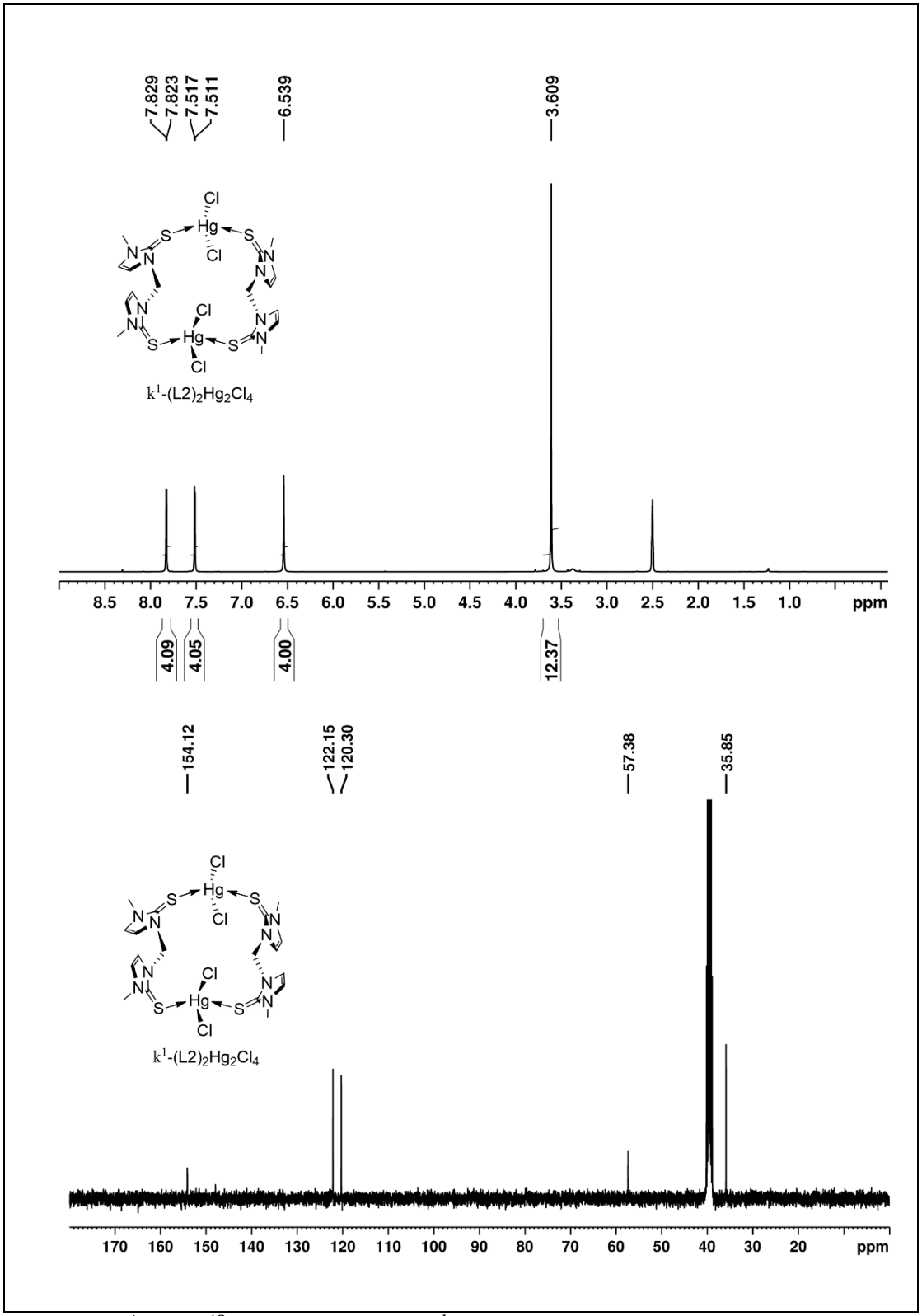

Figure S20. ^{1}H and ^{13}C NMR spectra of k^{1}-$(L2)_2Hg_2Cl_4$ in DMSO-d_6.

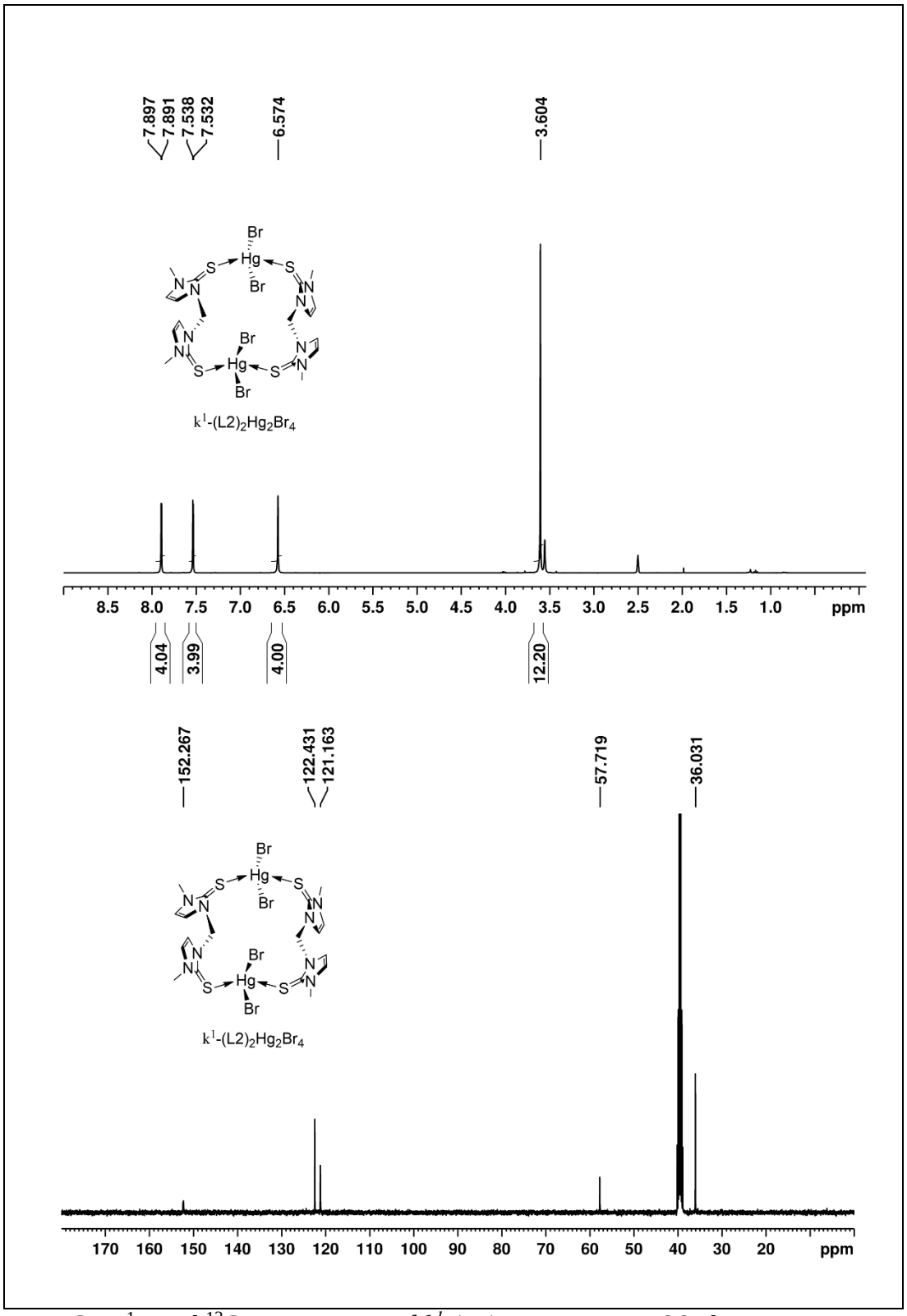

Figure S21. ^{1}H and ^{13}C NMR spectra of k^{1}-$(L2)_2Hg_2Br_4$ in DMSO-d_6.

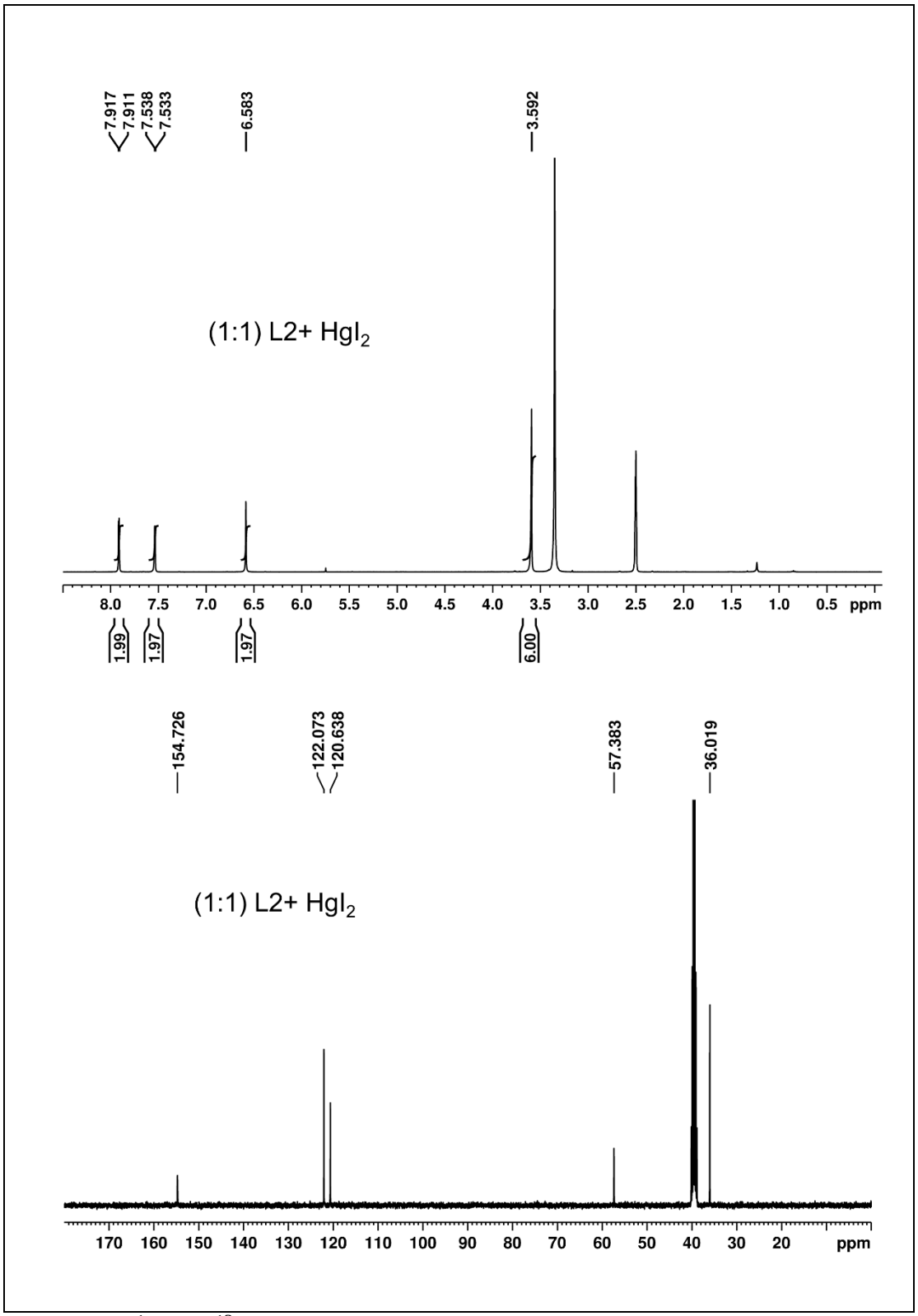

Figure S22. ^{1}H and ^{13}C NMR spectra of the solution containing L2 and HgI_2 in 1:1 molar ratio in DMSO-d_6.

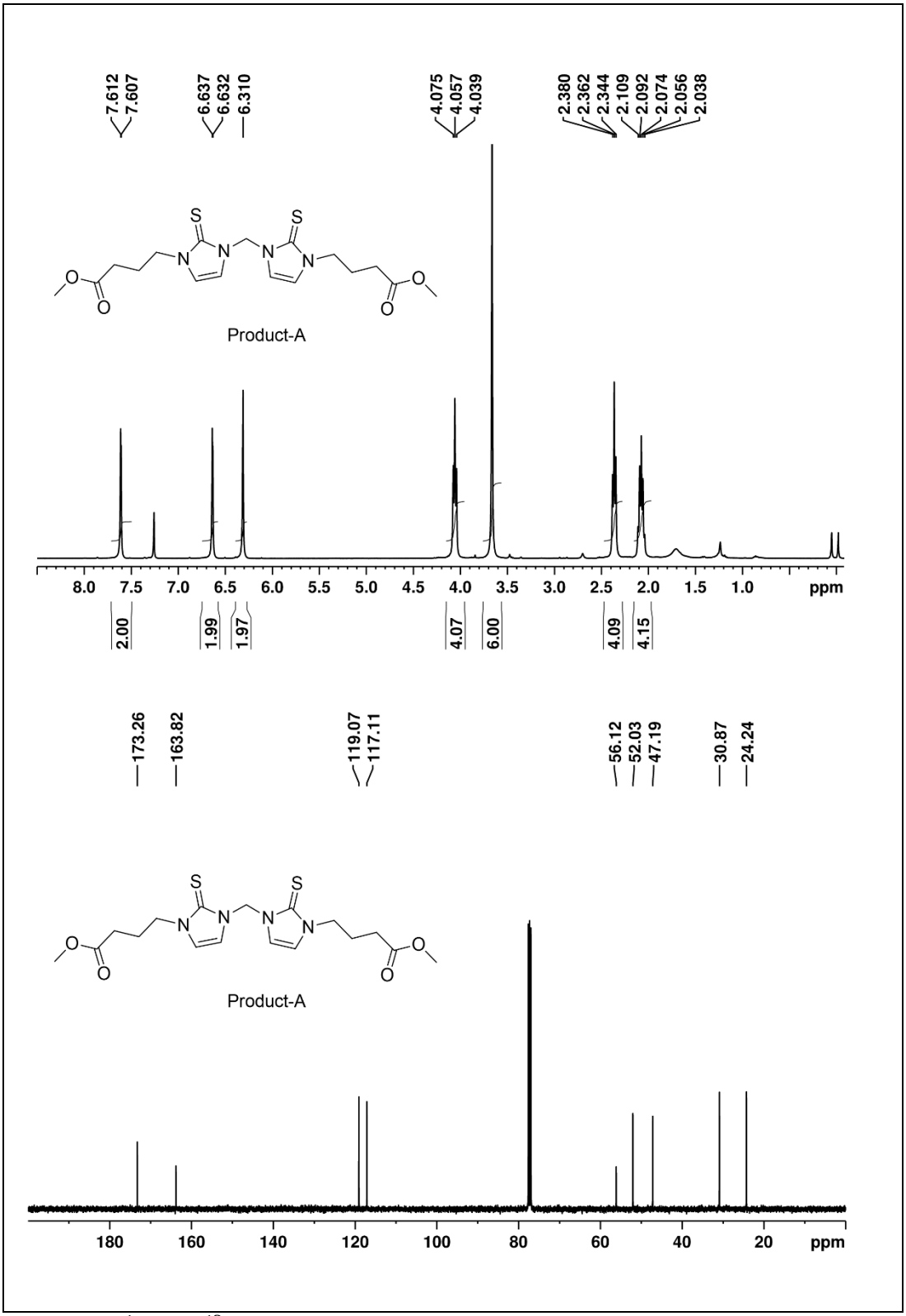

Figure S23. ^{1}H and ^{13}C NMR spectra of Product-A (L3-Ester) in DMSO-d_6.

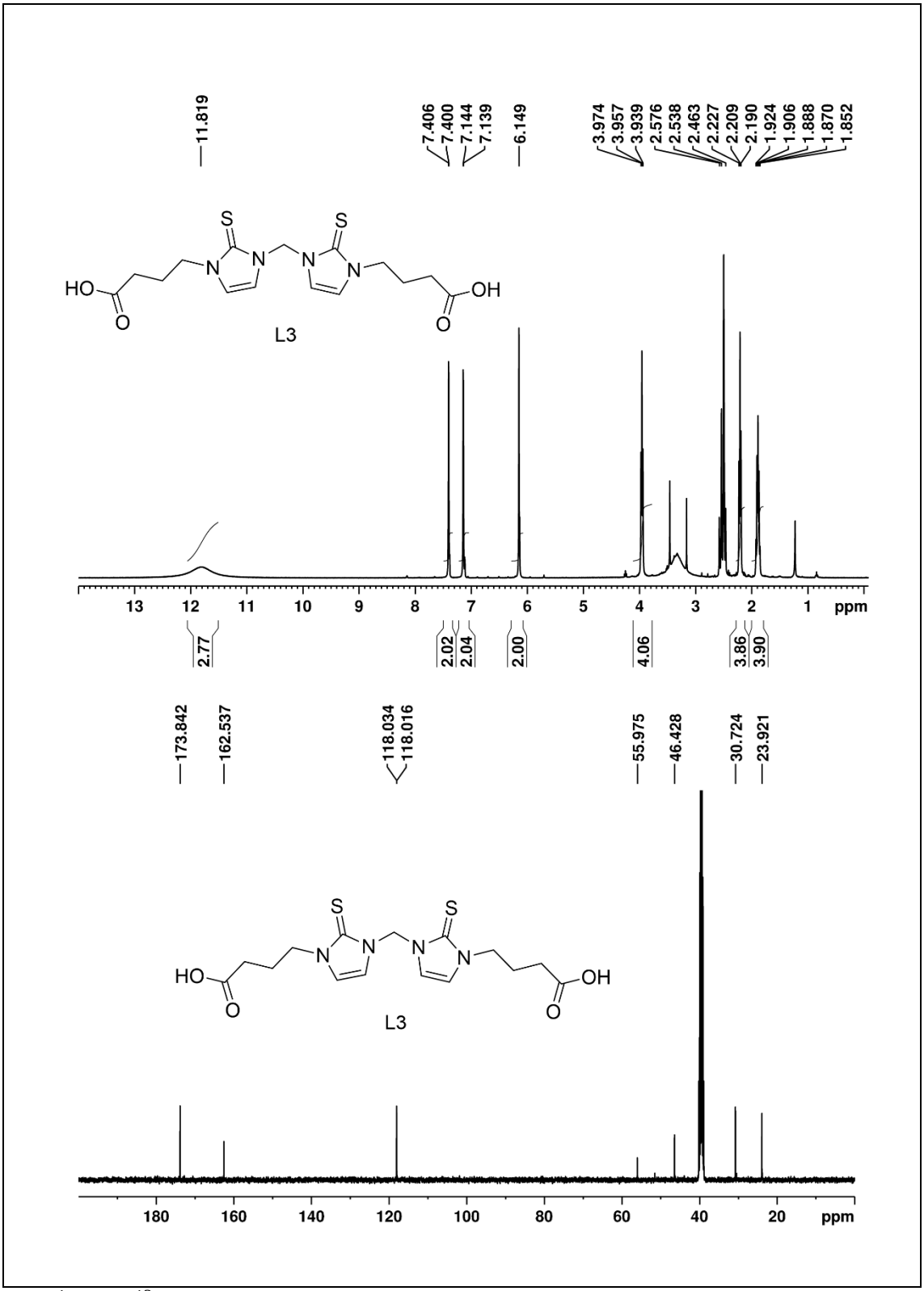

Figure S24. ^{1}H and ^{13}C NMR spectra of L3 in DMSO-d_6.

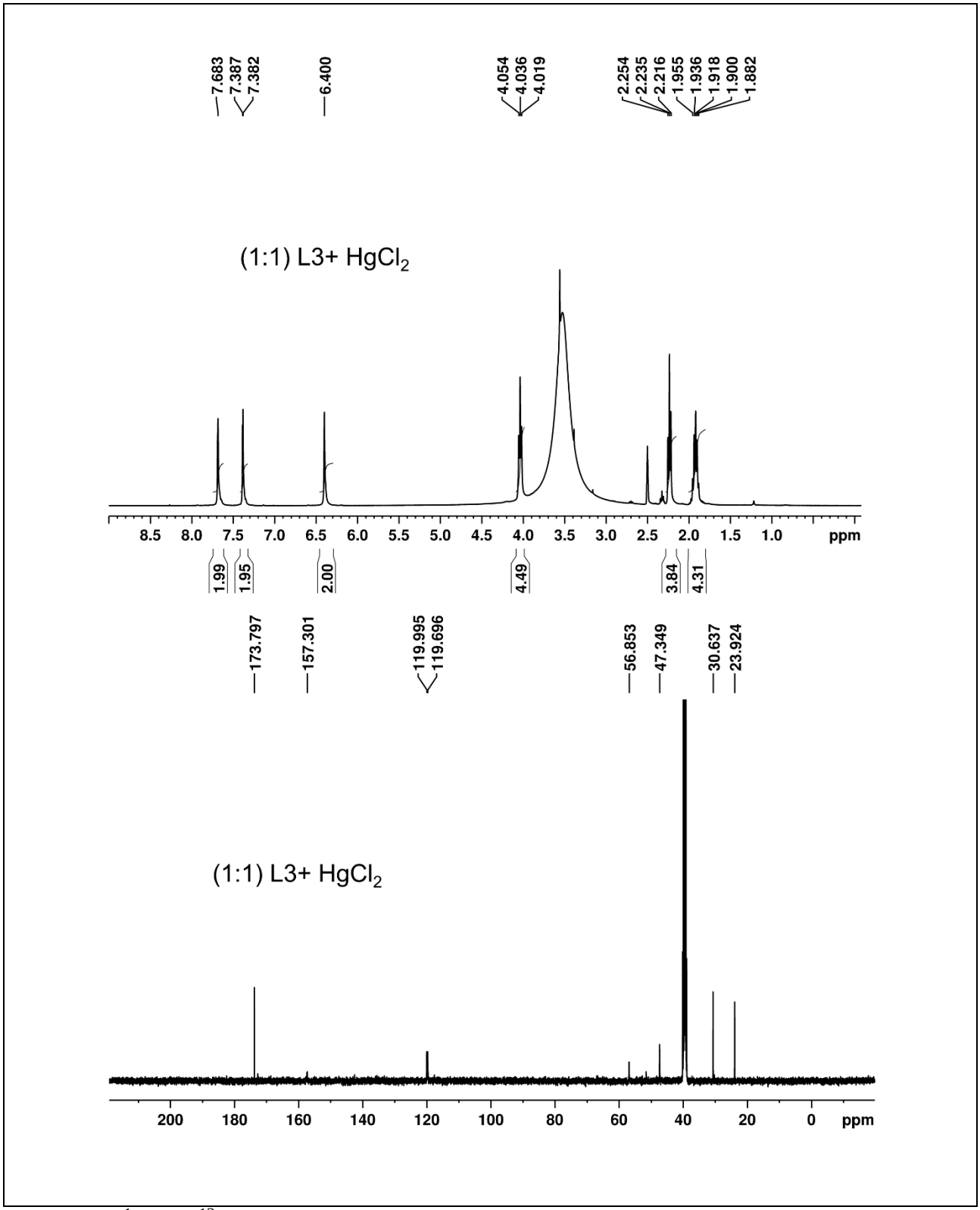

Figure S25. ^{1}H and ^{13}C NMR spectra of the solution containing L3 and $HgCl_2$ in 1:1 molar ratio in DMSO-*d*$_6$.

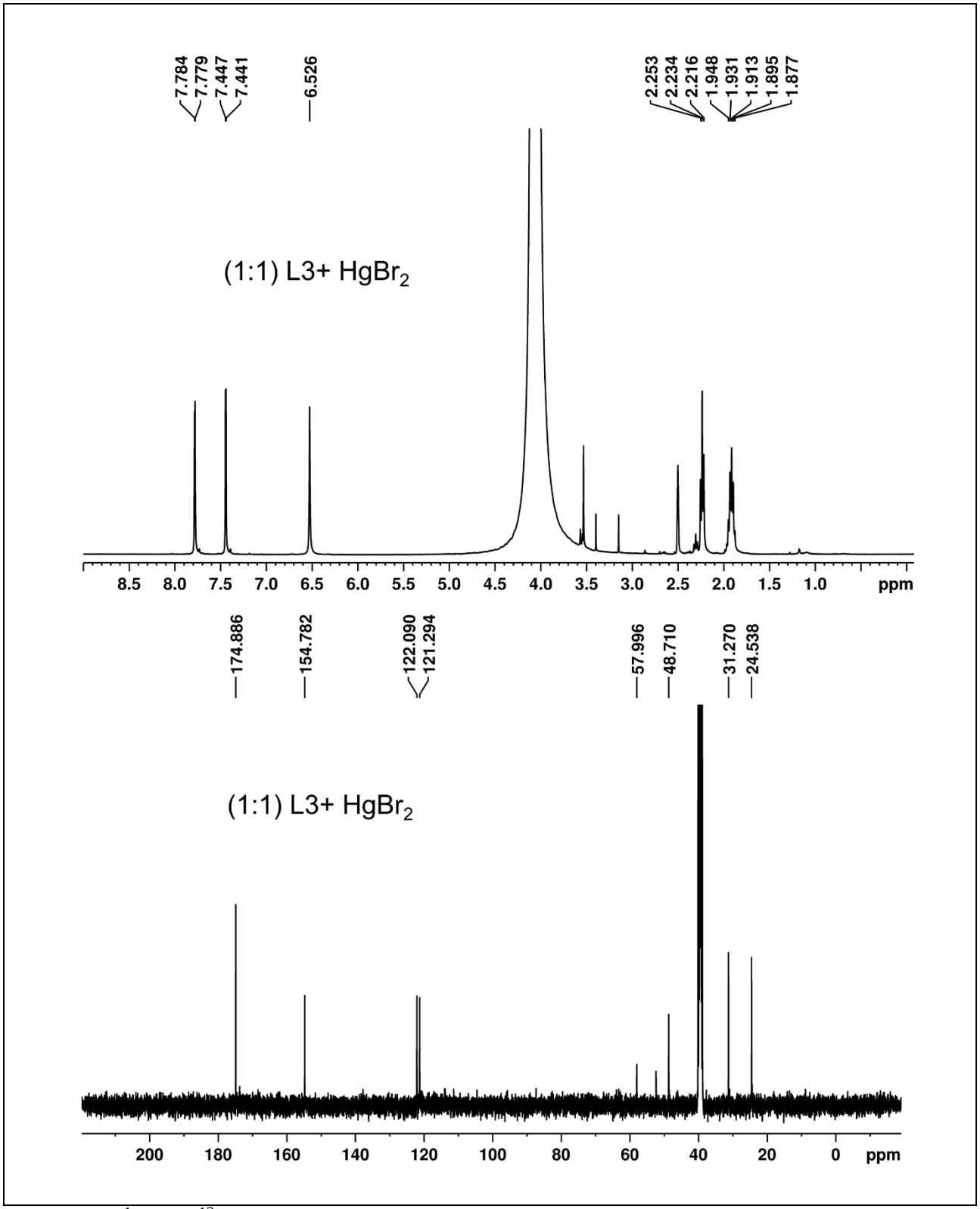

Figure S26. ^{1}H and ^{13}C NMR spectra of the solution containing L3 and $HgBr_2$ in 1:1 molar ratio in DMSO-d_6.

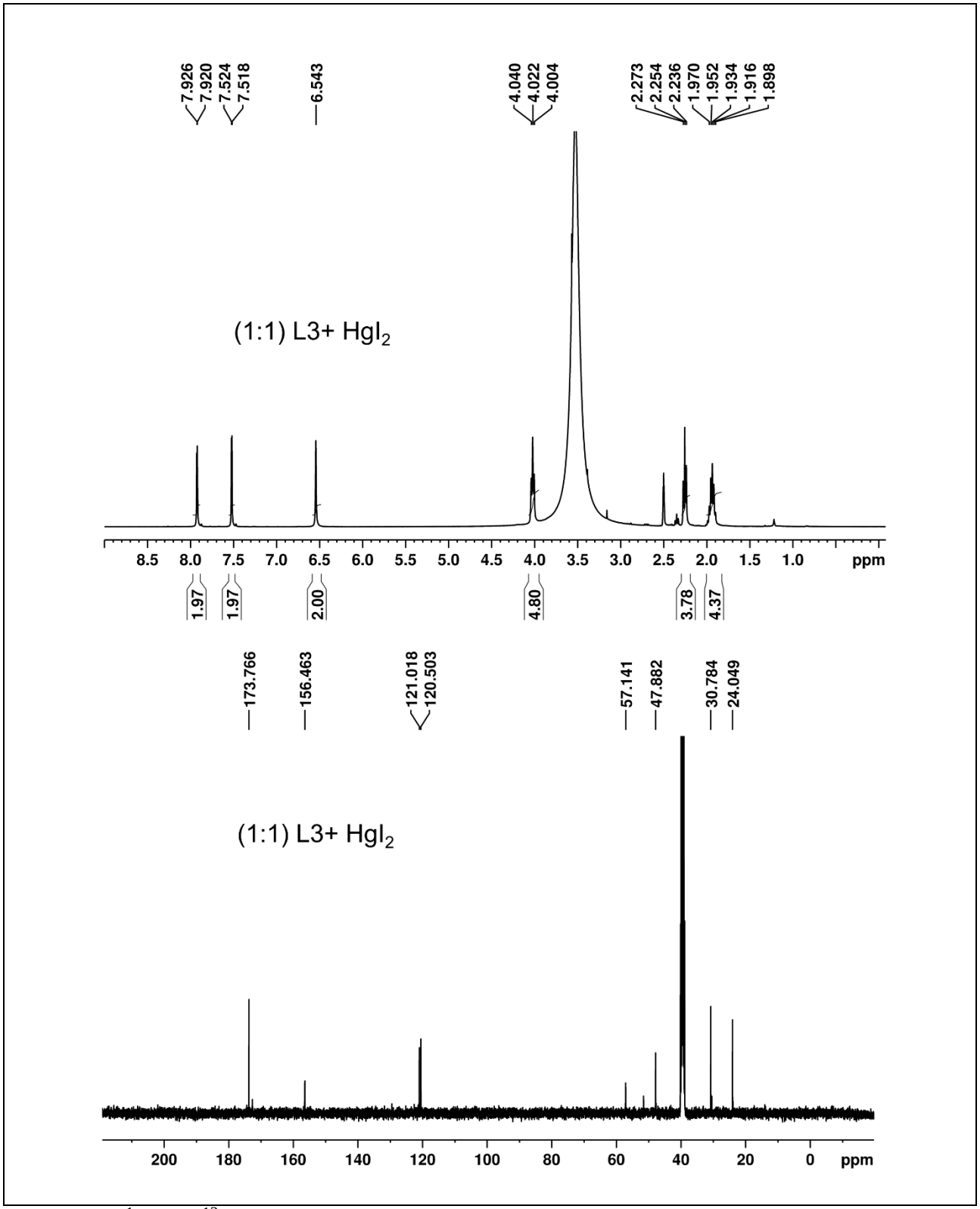

Figure S27. ^{1}H and ^{13}C NMR spectra of the solution containing L3 and HgI_2 in 1:1 molar ratio in DMSO-*d*$_6$.

7. Cell culture studies: For all the cell culture experiments, cells were grown in humidified 5% CO_2 incubator at 37 °C. All three ligands (L1, L2 and L3) were dissolved in incomplete media with 0.02% DMSO (to avoid any precipitation) to obtain final stock solution concentration of 100 μM. The 100 μM stock solution of $HgCl_2$ was also prepared in incomplete media. The cytotoxic profile of $HgCl_2$ on HepG2 cells are shown below, Figure S28.

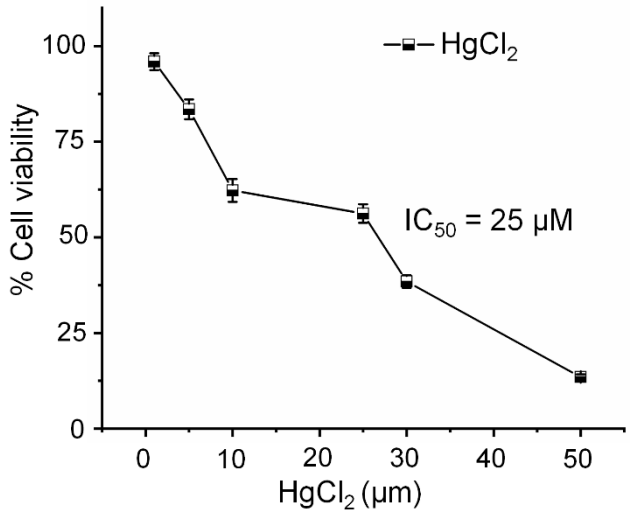

Figure S28. Percentage cell viability of HepG2 cells treated with $HgCl_2$ in various concentrations (5 –50 μM) 24 h by using MTT assay.

(a) Sample preparation for measurement of ligand internalization by HRMS: Cells ($1x10^5$) were grown by using T-75 flask in complete media and incubated under humidified 5% CO_2 incubator at 37 °C until the confluence reaches 80%. Then cells were treated with L3 ligand at a final concentration of 100 μM and incubated for 4 h in 5% CO_2 incubator at 37 °C. After incubation, the cells were washed thoroughly with cold PBS buffer solution (5 x 5 ml) followed by tripsinize and collect the cells by centrifugation to avoid the losing cells in washing process. The cells were re-suspended in PBS then lysed by probe sonication and supernatant was collected. The supernatant was analysed by using Agilent HRMS-QTOF (U.S.A) coupled to a UFLC system.

(b) Determination of ROS by pretreatment of ligand: The intracellular protective effect of L3 against $HgCl_2$ induced toxicity was estimated by measurement of ROS production by using DCFH-DA assay. In details, the cells $1x\ 10^6$ were seeded into three 6-well plate and incubated with 100 μM of L3 for 4 h, 12 h and 24 h under 5% CO_2 at 37 °C.

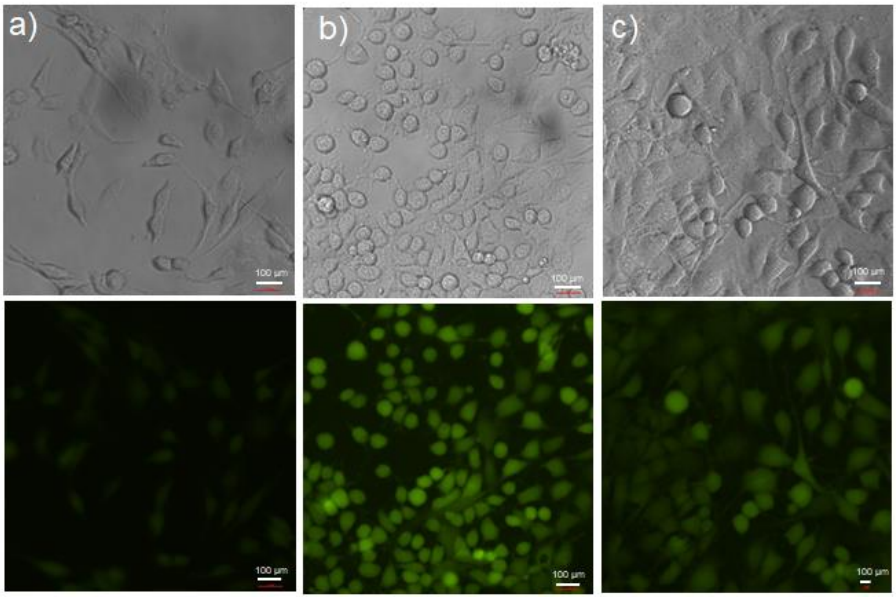

Figure S29. Bright field (TOP) and the corresponding fluorescence images (bottom) of untreated (a), 20 µM $HgCl_2$ (b), 20 µM $HgCl_2$ + 100 µM L3 (24 h pretreatment of L3).

After incubation, the media was removed and then cells were further treated with 20 µM of $HgCl_2$, dissolved in complete media, in fresh media and incubated for 4h. After 4h, the cells were treated with 5 µM of DFCH-DA and incubated for another 30 min in 5% CO_2 incubator at 37 °C. Then the cells were washed with PBS and proceed for determination of ROS levels under Nikon fluorescence microscopy at excitation wavelength at 488 nm and emission wavelength at 525 nm (Figure S28) and measured the mean intensity profile of L3 with various incubation time intervals as shown in Figure S29.

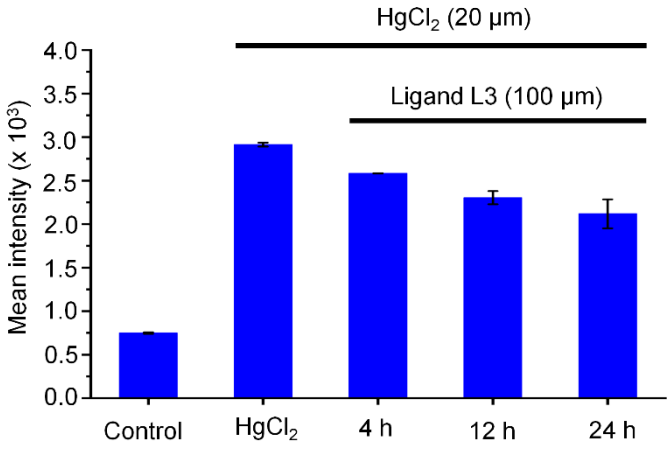

Figure S30. The relative mean intensity profile of ROS production in HepG2 cells treated with $HgCl_2$ and pre-treated with L3 for 4 h, 12 h, and 24 h followed by treatment of $HgCl_2$ for 2 h.

8. References:

(1) Frisch, M. J.; Trucks, G. W.; Schlegel, H. B.; Scuseria, G. E.; Robb, M. A.; Cheeseman, J. R.; Scalmani, G.; Barone, V.; Mennucci, B.; Petersson, G. A.; Nakatsuji, H.; Caricato, M.; Hratchian, X. Li, H. P.; Izmaylov, A. F. Bloino, J.; Zheng, G.; Sonnenberg, J. L.; Hada, M.; Ehara, M.Toyota, K.; Fukuda, R.; Hasegawa, J.; Ishida, M.; Nakajima, T.; Honda, Y.; Kitao, O.; Nakai, H.; Vreven, T.; Montgomery, J. A; Peralta, Jr., J. E.; Ogliaro, F.; Bearpark, M.; Heyd, J. J.; Brothers, E.; Kudin, K. N.; Staroverov, V. N.; Kobayashi, R.; Normand, J.; Raghavachari, K.; Rendell, A.; Burant, J. C.; Iyengar, S. S.; Tomasi, J.; Cossi, M.; Rega, N.; Millam, J. M.; Klene, M.; Knox, J. E.; Cross, J. B.; Bakken, V.; Adamo, C.; Jaramillo, J.; Gomperts, R.; Stratmann, R. E.; Yazyev, O.; Austin, A. J.; Cammi, R.; Pomelli, C.; Ochterski, J. W.; Martin, R. L.; Morokuma, K.; Zakrzewski, V. G.; Voth, G. A.; Salvador, P.; Dannenberg, J. J.; Dapprich, S.; Daniels, A. D.; Farkas, O.; Foresman, J. B.; Ortiz, J. V.; Cioslowski, J.; Fox, D. J.; Gaussian 09, revision D.01; Gaussian, Inc.: Wallingford, CT, 2009.